Running Head: Tonoplast aquaporins and lateral root development

Corresponding authors: François Chaumont

Institut des Sciences de la Vie

Université catholique de Louvain

Croix du Sud 4-L7.07.14

B-1348 Louvain-la-Neuve

Belgium

Phone number: +32 10 478485

E-mail address: francois.chaumont@uclouvain.be

Research Area:

Cell Biology

Genes, Development and Evolution

Tonoplast aquaporins facilitate lateral root emergence

Hagen Reinhardt, Charles Hachez, Manuela Désirée Bienert, Azeez Beebo, Kamal Swarup, Ute Voß, Karim Bouhidel, Lorenzo Frigerio, Jan K. Schjoerring, Malcolm J. Bennett, Francois Chaumont

Institut des Sciences de la Vie, Université catholique de Louvain, Croix du Sud 4-L7.07.14, B-1348 Louvain-la-Neuve, Belgium (H.R., C.H., F.C.); Department of Plant and Environmental Sciences, Faculty of Sciences, University of Copenhagen, Thorvaldsensvej 40, DK-1871 Frederiksberg C, Denmark (M.D.B., J.K.S.); Université de Bourgogne, UMR1347 Agroécologie IPM, BP 86510, F-21000 Dijon, France (A.B., K.B.); Centre for Plant Integrative Biology, University of Nottingham, LE12 5RD, UK (K.S., U.V., M.B.); School of Life Sciences, University of Warwick, Coventry CV47AL, UK (L.F.)

Summary

Aquaporins located in the vacuolar membrane contribute to the proper development of lateral roots

Footnotes:

This work was supported by grants from the Belgian National Fund for Scientific Research (FNRS), the Interuniversity Attraction Poles Programme-Belgian Science Policy (IAP7/29) and the Belgian French community ARC11/16-036 project. HR was a Research Fellow at the "Fonds pour la Formation à la Recherche dans l'Industrie et dans l'Agriculture".

Present address:

H.R.: Max-Planck-Institute for Plant Breeding Research, Carl-von-Linne-Weg 10, 50829 Cologne, Germany

A.B.: Department of Biological and Environmental Sciences, University of Gothenburg, Box 461, 405 30 Gothenburg, Sweden

C.H. and M.D.B. contributed equally to the work.

Corresponding author: François Chaumont (e-mail: francois.chaumont@uclouvain.be)

Abstract

Aquaporins (AQPs) are water channels allowing fast and passive diffusion of water across cell membranes. It was hypothesized that AQPs contribute to cell elongation processes by allowing water influx across the plasma membrane and the tonoplast in order to maintain adequate turgor pressure. Here, we report that, in *Arabidopsis thaliana*, the highly abundant tonoplast AQP isoforms AtTIP1;1, AtTIP1;2 and AtTIP2;1 facilitate the emergence of new lateral root primordia (LRP). The number of lateral roots was strongly reduced in the triple *tip* mutant, whereas the single, double and triple *tip* mutants showed no or minor reduction in growth of the main root. This phenotype was due to the retardation of LRP emergence. Live cell imaging revealed that tight spatio-temporal control of TIP abundance in the tonoplast of the different LRP cells is pivotal to mediating this developmental process. While lateral root emergence is correlated to a reduction of AtTIP1;1 and AtTIP1;2 protein levels in LRPs, expression of AtTIP2;1 is specifically needed in a restricted cell population at the base, then later at the flanks, of developing LRPs. Interestingly, the LRP emergence phenotype of the triple *tip* mutants could be fully rescued by expressing *AtTIP2;1* under its native promoter. We conclude that TIP isoforms allow the spatial and temporal fine-tuning of cellular water transport which is critically required during the highly regulated process of LRP morphogenesis and emergence.

Introduction

Plant cell elongation is a developmental process during which cells increase 10- to 100-fold in volume before reaching their final size. It requires a fast and continuous inflow of water, which ends up mainly in the vacuole, in a process which is controlled by gradients in water potential, which itself is generated by the accumulation of solutes (for review, see (Fricke and Chaumont, 2007)).

The fast and passive movement of water across cell membranes is facilitated by the presence of water channels, called aquaporins (AQPs), which belong to the superfamily of the Major Intrinsic Proteins (MIPs) (Agre et al., 1993; Maurel, 1997; Gomes et al., 2009). AQPs are involved, on the one hand, in the long-distance movement of water during evapo-transpiration and, on the other hand, in the short-distance transport and osmotic adjustment within cells (expansion, opening of stomata, water homeostasis) (Maurel et al., 2008; Gomes et al., 2009; Heinen et al., 2009; Chaumont and Tyerman, 2014). They also contribute to the maintenance of a favourable water balance within plants under changing and sometimes hostile environmental conditions. Several AQPs are also important for the facilitated membrane diffusion of other uncharged solutes such as urea, CO_2, NH_3, H_2O_2 and metalloids (Liu et al., 2003; Uehlein et al., 2003; Jahn et al., 2004; Bienert et al., 2007; Bienert et al., 2008; Bienert et al., 2011; Bienert et al., 2014).

The genome of *Arabidopsis thaliana* encodes 35 MIPs that phylogenetically cluster in four subfamilies: Plasma membrane Intrinsic Proteins (PIPs), Tonoplast Intrinsic Proteins (TIPs), Small basic Intrinsic Proteins (SIPs) and Nodulin 26-like Intrinsic Proteins (NIPs) (Johanson et al., 2001). Arabidopsis AtTIPs (10 isoforms) and AtPIPs (13 isoforms) are mostly found in the vacuolar and plasma membrane, respectively, and act as water channels when heterologously expressed in *Xenopus* oocytes (Maurel et al., 1993; Daniels et al., 1994; Kammerloher et al., 1994; Maurel et al., 1995; Daniels et al., 1996; Weig et al., 1997; Johanson et al., 2001). The TIP protein sequences are more divergent compared to PIPs and phylogenetically divided into five groups (TIP1-5). TIP1 and TIP2 isoforms are largely expressed in vegetative tissues and are thought to be preferentially associated with the large lytic vacuoles and vacuoles accumulating vegetative storage proteins, respectively (Jauh et al., 1998). TIP3s are expressed in seeds (Vander Willigen et al., 2006; Hunter et al., 2007; Frigerio et al., 2008) and TIP5;1 is exclusively expressed in dry seeds and pollen grains (Vander Willigen et al., 2006; Soto et al., 2008; Wudick et al., 2014).

The importance of TIP AQPs in tissue elongation has been mainly suggested by transcriptional analysis. Arabidopsis plants expressing the β-glucuronidase marker protein under the transcriptional control of the *AtTIP1;1* promoter show high GUS activity in root and stem elongating tissues, but no expression is detected in meristems or older parts of plants (Ludevid et al., 1992). The maize ZmTIP1;1 homologue is highly expressed in expanding cells in roots, leaves and reproductive organs (Barrieu et al., 1998; Chaumont et al., 1998). An increased expression of *TIP*s is also observed in elongating tissues of hypocotyls in soybean, castor bean and radish seedlings (Higuchi et al., 1998; Suga et al., 2001; Eisenbarth and Weig, 2005) and in protruding seed radicles in canola (Gao et al., 1999). Furthermore, the abundance of *HvTIP1;1* mRNA increases in the barley slender mutant, which exhibits a faster leaf elongation rate compared to the wild-type (Schunmann and Ougham, 1996). However, even if the expression pattern of these *TIP* genes suggests an important role in cell elongation, direct proof of this physiological function during plant development is still missing. Some clues come from the overexpression of the cauliflower or tobacco *TIP1;1* gene in tobacco suspension cells, which results in an increase in cell growth and size (Reisen et al., 2003; Okubo-Kurihara et al., 2009).

Roots represent a very useful model to investigate cell elongation and growth processes (De Smet et al., 2012; Petricka et al., 2012). The primary root meristem, located at the organ apex, continuously produces cells that elongate after they leave the apical meristem and, hence, push the meristem forward. The primary root of many dicotyledonous plants repeatedly branches to generate several orders of lateral roots. In Arabidopsis, lateral roots exclusively originate from three files of pericycle founder cells overlaying the xylem poles (Dolan et al., 1993). Xylem-pole pericycle cells are first 'primed' to become lateral root founder cells close to the apical meristem in a zone termed the basal meristem (De Smet et al., 2007). Lateral roots are initiated when pairs of pericycle founder cells undergo several rounds of anticlinal division to create a new lateral root primordium (LRP) composed of up to ten cells of equal length designated as stage I (Malamy and Benfey, 1997; Casimiro et al., 2001; Dubrovsky et al., 2001). Next, these cells divide periclinally, giving rise to an inner and an outer layer (termed stage II). Further anticlinal and periclinal divisions create a dome-shaped primordium (stages III to VII) that emerges (stage VIII) from the parental root (Malamy and Benfey, 1997; Peret et al., 2009). The tight correlation of lateral root formation and emergence is controlled by auxin, which acts as a local inductive signal that also triggers cell separation in the overlaying tissues (Swarup et al., 2008).

The involvement of PIP AQPs in proper lateral root emergence (LRE) was recently demonstrated in Arabidopsis (Peret et al., 2012). Expression analysis revealed that most of the analyzed *AtPIP* and *AtTIP* genes are repressed during LRP formation, a regulatory response that can be mimicked by exogenous treatment with auxin. The latter effect is correlated with a reduction in cell and whole root hydraulic conductivity. *AtPIP2;1* overexpressing lines and *Atpip2;1* knock-out mutants exhibit delayed LRE, with an accumulation of early LRP developmental stages at 42 h after a gravitropic stimulus. Furthermore, LRPs fail to protrude into the overlaying tissues (Peret et al., 2012). This pattern of delayed LRP development and emergence in both *AtPIP2;1* overexpressing lines and *Atpip2;1* mutants was predicted by a mathematical model. The interplay of the spatial and temporal control of auxin-dependent cell hydraulic conductivity could be critical during LRP development.

In this work, we investigated the contribution of AtTIP AQPs in this developmental process making use of different *tip* knock-out lines. While the simultaneous lack of *AtTIP1;1*, *AtTIP1;2* and *AtTIP2;1* had only a small impact on the primary root growth, it delayed LRE resulting in a strong reduction in lateral root number. The phenotype could be fully rescued by expressing *AtTIP2;1* under its native promoter. These results show that regulation of the tonoplast water permeability plays, in addition to the plasma membrane permeability, an important role in early lateral root growth and development.

Results

Molecular analysis of the *tip* knock-out lines

To gain insight into TIP function, different Arabidopsis lines with T-DNA or transposon insertion in *AtTIP1;1*, *AtTIP1;2* and *AtTIP2;1* genes were characterized. For all *tip* mutant lines, the homozygosity of the insertions was confirmed by PCR using gene-, T-DNA- or transposon-specific primers (Table S1). The T-DNA and dSpm insertions in single *tip1;1*, *tip1;2* and *tip2;1* mutants are illustrated in Supplemental Fig. 1A, B and C, respectively. The *tip1;2 x tip2;1* double mutant was obtained by crossing the two single insertion lines (Supplemental Fig. 1B and C). The *tip1;1 x tip1;2 x tip2;1* triple was obtained by crossing independent *tip* single mutants (Supplemental Fig. 1D) which contain insertion at different positions in the *AtTIP* genes compared to the single *tip* mutant lines used in this study (as shown in Supplemental Fig. 1A, B, and C) (Schussler et al., 2008). RT-PCR confirmed the absence of the corresponding RNA in the single, double and triple *tip* mutant lines (Supplemental Fig. 1).

The *tip* mutant lines did not exhibit any striking phenotypes when grown under standard conditions (data not shown). To investigate whether this observation was due to compensatory up-regulation of other *AtTIP* genes, we analysed the mRNA levels of all the *AtTIP* isoforms in roots and shoots of 12 day-old wild-type and *tip* mutant seedlings by RT-qPCR using isoform-specific primers (Table S1). In both roots and leaves, the transcript levels of the *AtTIP* genes carrying T-DNA or transposon insertion were down-regulated by at least ~64-fold compared to the wild-type (Fig. 1). The *AtTIP* expression profile of the detected isoforms in the wild-type corresponded to those shown in the literature (Alexandersson et al., 2005; Schussler et al., 2008). In roots, no significant upregulation of the root expressed genes (*AtTIP1;1, AtTIP1;2, AtTIP2;1, AtTIP2;2, AtTIP2;3 and AtTIP4;1*) was observed in the *tip* mutant lines, except for the *tip1;2* mutant in which *AtTIP2;1* exhibited a 3-fold upregulation (Fig. 1). *AtTIP1;3*, *AtTIP3;1*, *AtTIP3;2* and *AtTIP5;1* transcripts could not be detected in wild-type or any of the *tip* mutant lines, confirming previous root expression data (Alexandersson et al., 2005).

The *tip* triple mutant exhibits shorter roots at 11 dag

Since *AtTIP* genes are expressed in elongation zones, the lack of the most highly expressed isoforms could result in a deficiency in cell elongation. As we did not observe any difference in hypocotyl elongation between the different *tip* mutant lines compared to the wild

type (data not shown), we decided to focus on root growth. No root growth phenotype was previously reported for *tip1;1* (Schussler et al., 2008; Beebo et al., 2009) and *tip1;2* (Schussler et al., 2008) single mutants, suggesting a possible functional redundancy of *AtTIP* isoforms. However, if *AtTIP*s are important for root growth processes, coinciding mutations in several *AtTIP* isoforms might cause growth phenotypes. Seedlings of the single *tip1;1,* double *tip1;2 x tip2;1* and triple *tip1;1 x 1;2 x 2;1* mutants were grown on vertical ½ MS plates containing 1.5 % sucrose and the elongation of the main root was monitored during seven days (see Materials and Methods). No significant difference in root length of double and triple mutants was observed compared to wild-type plants at 7 days after germination (dag) (Fig. 2). However, the *tip1;1* single mutant exhibited a small but significant increase in root length compared to the wild-type at early seedling stage (up to 6 dag).

Since cell elongation is driven by high and constant cell turgor, which is obtained by high osmotic concentration of the vacuolar sap, changes in turgor pressure mediated by an osmotic stress alter elongation processes (Fricke and Peters, 2002). Therefore, we investigated root elongation of *tip* mutants under osmotic stress conditions. At 7 dag, the seedlings from the experiment shown in Fig. 2A were transferred to plates containing ½ MS medium supplemented with 0, 200 or 400 mM mannitol, in the absence or presence of 1.5 % sucrose. Sucrose itself could induce an osmotic stress on the seedlings and mask effects by the supplemented mannitol (1.5 % sucrose correspond to about 44 mM, exhibiting an osmotic pressure of about 0.11 MPa according to van't Hoff's law). The root length was measured as described above. To avoid variations resulting from different root lengths of individual seedlings at the time of the transfer, the position of the root tip after the transfer was set to zero and the increase in length after the transfer was measured. No significant difference in root length increase was observed for all *tip* mutants compared to wild-type, when they were transferred to plates containing 0, 200 or 400 mM mannitol without sucrose (Fig. 2). In the presence of 1.5 % sucrose, but absence of mannitol (i.e. under control conditions), only the *tip1;1 x 1;2 x 2;1* triple mutant exhibited a significant lower increase in root length compared to WT four days after the transfer (corresponding to 11 dag). In the presence of 400 mM mannitol and 1.5 % sucrose, all the *tip* mutant lines showed significant shorter roots after the transfer.

The *tip* triple mutant exhibits significantly less lateral roots

Since the triple *tip* mutant line had shorter roots at 11 dag under control conditions, we selected this line for a closer investigation of its root phenotype. Arabidopsis wild-type and

tip1;1 x 1;2 x 2;1 mutant plants were grown on vertical plates containing ½ MS medium supplemented with 1.5 % sucrose. Twelve days after germination, the length of the main roots was measured, and the lateral roots were counted (Fig. 3). The triple *tip* mutant exhibited slightly shorter roots (Fig. 3A and B, about 10 % reduction) confirming our previous observations (Fig. 2B). Interestingly, the triple mutant exhibited a 50 % reduction in the number of lateral roots compared to wild-type (Fig. 3A and C). The length of all lateral roots was measured for 50 plants from each genetic background, by drawing a straight line between the tip and the base of individual lateral roots. Whereas the number of lateral roots with a length higher than 3.0 mm was fairly similar between wild-type and the triple *tip* mutant lines, the latter exhibited a reduced number of newly emerged (short) lateral roots (Fig. 3D), suggesting a defect during early stages of lateral root development. The reduced number of lateral roots in the triple *tip* mutant was observed on sucrose containing medium, which was previously shown to promote outgrowth of initialised LRPs (Macgregor et al., 2008).

Disrupted *AtTIP* expression causes delayed LRP development

To determine the contribution of the *AtTIP* genes during early stages of LRP development, we induced lateral root initiation employing a 90° gravitropic stimulus, which is commonly used to synchronize LR initiation and investigate its developmental progression (Fig. 4) (Ditengou et al., 2008; Lucas et al., 2008; Richter et al., 2009; Peret et al., 2012). Since sucrose contained in the culture medium can promote LRP development (Macgregor et al., 2008), we performed this experiment on sucrose-free medium to strengthen LRP phenotype of the *tip* mutants. In this analysis, in addition to the triple *tip* mutant, we included the single *tip1;1*, *tip1;2*, *tip2;1* and double *tip1;2 x tip2;1* mutant lines to possibly relate the contribution of single *AtTIP* isoform to LRP development, even if no phenotype regarding lateral roots was previously reported for *tip1;1*, *tip1;2* and *tip1;1 x tip1;2* mutants (Schussler et al., 2008; Beebo et al., 2009). To date no phenotypic data are available for the *tip2;1* mutant line.

In wild type plants, stage I primordia were first detected 18 h post-gravitropic induction (pgi) and the other stages (II-VIII) peaked approximately every 3 h until emergence (stage Em) at 42 h pgi (Peret et al., 2012). At 18 h pgi, no significant difference in LRP stage distribution was detected in single, double or triple *tip* mutants compared to wild type (Fig. 4B), indicating that these *AtTIP* genes were not required for primordia initiation. In contrast, at 42 h pgi, all the *tip* mutant lines showed a shift in LRP stage distribution towards

earlier stages (Fig. 4C). Whereas ~50 % of LRPs had emerged in wild-type roots, only 5 to 15 % of the lateral roots at the bending site of *tip* mutants had emerged. In some seedlings of the *tip1;2 x tip2;1* and *tip1;1 x tip1;2 x tip2;1* mutants, LRPs still remained in stage II, in contrast to the wild-type plants where the earliest LRP stage found was V. These data strongly indicate an important role of *AtTIP*s in LRP development. The non-additive response of the single, double and triple mutant lines suggests a complex interplay of different AtTIP isoforms during this process.

To verify that the delay in LRP development was due to the T-DNA or transposon insertion in *AtTIP* genes, we included another independent batch of single *tip* mutants in our analysis, *tip1;1-2*, *tip1;2-2* (Schussler et al., 2008) and *tip2;1-2*, which were used to obtained the triple *tip* mutant. The T-DNA or transposon insertions in these lines were verified by PCR on genomic DNA (Supplemental Fig. 2). These new single *tip* mutated lines were subjected to a root bending assay. All of them except the *tip1;2-2* line showed a similar delay in LRP development at 42 h pgi (Supplemental Fig. 2) as the previously tested lines (Fig. 4B).

AtTIP expression patterns is correlated to lateral root formation

A strictly defined spatial and temporal TIP expression pattern might be crucial for the directed growth of complex three dimensional structures, such as LRPs. During LRE, cells located in the outer layers of the LRP base need to stretch as the LRP increases in volume, suggesting that requirement for a faster water influx across the plasma membrane into the cytosol as well as across the tonoplast into the vacuole, which occupies most of the volume in these cells. It was previously reported that the expression of *AtTIP1;1*, *AtTIP1;2, AtTIP2;2* and *AtTIP2;3* was rapidly down-regulated after lateral root gravitropic induction (Peret et al., 2012). To investigate the expression pattern of AtTIP1;1 and AtTIP1;2 in developing LRPs, roots from 5- to 7-day old seedlings containing *proAtTIP1;1::AtTIP1;1-GFP* or *proAtTIP1;2:AtTIP1;2-GFP* constructs were stained for 5 min with propidium iodide and LRPs were investigated using confocal laser scanning microscopy (Fig. 5). The expression of AtTIP1;1-GFP (Fig. 5A-H) and AtTIP1;2-GFP (Fig. 5I-P) under their native promoter appeared to be ubiquitous in the main root. In the zone where lateral root development occured, the TIP-GFP signals were abundant in the outer cell layers facing the LRPs during early developmental stages (Fig. 5E-F and M-N, LRP stages II and IV) but were reduced in these cells at late developmental stages (Fig. 5G-H and O-P, LRP stages VI and emerged). No expression of AtTIP1;1-GFP or AtTIP1;2-GFP was detected in LRPs perfectly correlating with the decrease in *AtTIP1;1* and *AtTIP1;2* mRNA levels measured during LRP development

(Peret et al., 2012). In addition, while the AtTIP1;2-GFP signal decreased in the cortex cells facing the LRPs during late developmental stages, it increased in the lateral root inner basal tissues and in the stele (Fig. 5O-P).

As no data was available for *AtTIP2;1* mRNA levels during LRP development, we used RT-qPCR to analyse the expression of *AtTIP2;1* in micro-dissected root bends in response to a gravitropic stimulus (Fig. 6). The level of *AtTIP2;1* mRNA increased 1.7 fold at 6 h pgi compared to time 0, and then dramatically decreased at 12 h pgi (Fig. 6A). This expression pattern differs from the one reported for *AtTIP1;1*, *AtTIP1;2, AtTIP2;2* and *AtTIP2;*3 but is similar to the expression of *AtPIP2;4* and *AtPIP2;1* (Peret et al., 2012).

To gain further insight on the expression pattern of AtTIP2;1 and given that AtTIP2;1-YFP expressed under the control of the *AtTIP2;1* promoter is detected in a ring-like cell cluster at the base of emerging lateral roots (Gattolin et al., 2009), we decided to closely investigate AtTIP2;1 expression during LRP development using the same translational reporter. Roots from 5- to 7-day old seedlings expressing the *proAtTIP2;1:AtTIP2;1-YFP* construct were stained for 5 min with propidium iodide and LRPs were investigated using confocal laser scanning microscopy. The expression of AtTIP2;1-YFP was exclusively restricted to sites of LRP development (Figs. 6 and 7). In LRPs at developmental stage II, no YFP fluorescence was detected (Fig. 6B and F) whereas, in LRPs at stage IV, a fluorescent signal was observed in a single cell file located in the pericycle of the newly established LRP (Fig. 6C, G, J). At stage VI, AtTIP2;1-YFP was also detected in about two cell layers surrounding the base of the newly developed LRP (Fig. 6D, H, K). At stage VIII, several cell layers at the base of the LRP showed a YFP fluorescent signal that was more intense in the larger, triangular shaped cells at the borders of the LRP (Fig. 6E, I and L, indicated by arrows).

As the images shown in Fig. 6F-L resulted from a 3D reconstruction of single confocal images taken at sequential focus planes, denoted as X-Y in Fig. 7, we virtually cut this image stack orthogonally in Y-Z planes. This analysis allowed us to determine that, at stage IV of LRP development, AtTIP2;1-YFP was expressed in a row of cells inside of the endodermis, presumably corresponding to pericycle cells (Fig. 7B-H). In stage VI of LRP development, AtTIP2;1-YFP was also observed in endodermal cells at the ends of the LRP and in newly raised primordial cells located at the base of the LRP, facing cortical cells (Fig. 7I-O). These results indicate that LRE requires a tight regulation of AtTIP expression. In particular AtTIP2;1 activity seems to be required for the growth of LRP basal and border cells and the

regulation of LRP development and LRE of the main root. LRE appears also to be correlated to a reduction of AtTIP1;1 and AtTIP1;2 protein levels in the cortex cells.

The delay in LRP development of the triple *tip* mutant is only rescued when *AtTIP2;1* is expressed under its native promoter

To correlate the LRP phenotype to the lack of AtTIPs, we modulated AtTIP expression in these mutants by expressing the respective AtTIP isoform under the control of the constitutive CaMV 35S promoter in the *tip* mutant lines. (Fig. 8) For the double and the triple mutants only one of the *TIP* genes was expressed. The expression of the *AtTIP* genes in the *tip* mutated lines was verified by RT-qPCR (Fig. 8A). In all the retransformed lines we measured a higher level of the respective *AtTIP* mRNA compared to the mutant. The retransformed *tip* mutated lines were subjected to a root bending assay and the LRPs were analysed 42 h pgi (Fig. 8B). The introduction of a constitutively expressed TIP isoform in the *tip1;1*, *tip1;2* or *tip2;1* mutants did not lead to a reversion of the LRP development defect but, instead, to a stronger delay in this process compared to the *tip1;1*, *tip1;2* or *tip2;1* single mutants. No change in the pattern of LRP development was detected in the complemented *tip1;2 x 2;1* double mutant lines. Finally, the expression of *AtTIP1;2* in the *tip1;1 x tip1;2 x tip2;1* background resulted in a shift of the LRP stages distribution towards the one observed in wild-type. However, the distribution pattern of wild type LRP development could not be reached, probably due to the fact that a fine tuning of AtTIP expression could not be achieved using the constitutively active 35S promoter (as observed when *AtPIP2;1* expression was driven by the 35S promoter in a *Atpip2;1* mutant line; (Peret et al., 2012)).

As *AtTIP2;1* exhibits an exclusively LRP-related expression pattern, we decided to investigate the ability of this particular isoform to rescue the LRP phenotype in the triple *tip* mutant. We created transgenic triple *tip* mutant lines containing *proAtTIP2;1::AtTIP2;1* or *proAtTIP2;1::AtTIP2;1:GFP* constructs, subjected them to a root bending assay as described above (Fig. 9). Both, the non-fluorescent and the GFP-tagged AtTIP2;1 expressed under the native promoter completely restored the WT-like LRP development of the triple *tip* mutant. Altogether, these data suggest that a fine tuning of the spatio-temporal distribution (and activity) of AtTIP2;1 is needed to promote LRP development and that ectopic expression of any AtTIP does not rescue or even negatively impacts this developmental process.

Discussion

TIPs play a role in lateral root formation

In this study we show that TIP AQPs are essential for the proper development of LRPs. As TIPs are known to be efficient water channels (Maurel et al., 1993; Maurel et al., 1995; Daniels et al., 1996; Gerbeau et al., 1999), their presence in the tonoplast is expected to allow rapid water exchange between the vacuole and the cytoplasm, an important process during cell expansion, which is driven by the turgor pressure. Since the development of LRPs is a rapid process with a time scale of hours and requires a complex set of cell divisions and expansions, a tight control of TIP abundance and activity in the tonoplast of the different LRP cells is probably important for this developmental process.

In a recent study, Peret *et al*. (2012) showed a similar action of plasma membrane AQPs during lateral root development. The authors developed a computational model, which predicts the effect of changes in cell plasma membrane water permeability in different LRP tissues. This model did not include the possibility to distinguish between water fluxes across the plasma membrane and the tonoplast, therefore it likely also holds for water fluxes across the tonoplast. Indeed, regulation of turgor pressure involved water flows across the plasma membrane as well as the tonoplast, since the vacuole occupies the major volume of the cell. Comparing this process with an electrical circuit, PIPs in the plasma membrane and TIPs in the tonoplast act as serial conductors, allowing the fast water exchange between the apoplast, the cytosol, and the vacuole. If the conductance of one of these membranes is reduced by a decreased amount of functional AQPs located in the respective membrane, the turgor regulation is expected to be affected.

The plant hormone auxin is a key regulator of lateral root development (Peret et al., 2009). Xylem pole pericycle cells form LRPs after local auxin levels are elevated, triggering a series of asymmetric cell divisions (De Smet et al., 2007; Dubrovsky et al., 2008). Auxin also promotes the LRP emergence by triggering the expression of cell-wall remodelling genes in the overlaying tissues (Laskowski et al., 2006; Swarup et al., 2008; Kumpf et al., 2013; Lucas et al., 2013). The local distribution pattern of auxin is created by specialised efflux and influx transport proteins, which cause the accumulation of auxin at the apex and in the overlaying tissues of the LRP (Swarup et al., 2008). LRP emergence and the concomitant physical modification of the overlaying tissues must be tightly co-regulated. Peret *et al*. (2012) showed that auxin regulates the expression of plasma membrane AQPs, mostly by repressing their expression, and therefore decreasing tissue hydraulic properties, which facilitates LRP

emergence. These data suggest that auxin fine-tunes the spatial and temporal control of root tissue hydraulics through the regulation of AQP distribution. In their study, the authors also observed a decrease of expression of *AtTIP1;1*, *AtTIP1;2*, *AtTIP2;2* and *AtTIP2;3* genes upon LRP development. In the present work, we observed that the expression of *AtTIP2;1* is first up-regulated during early stages of LRP formation before subsequently being down-regulated, suggesting that AtTIP2;1 has a specific role during this process. However the RT-qPCR experiments reported in this study and in Peret et al. (2012) were performed from total root sections, which prevented to conclude about the exact location of AQP expression. Therefore, we analysed the expression of fluorescently-tagged TIP proteins expressed under the control of their own promoter (Fig. 5, 6 and 7). The absence of AtTIP1;1-GFP and AtTIP1;2-GFP proteins in the emerging LRP was in accordance with the decrease in mRNA level detected in RT-qPCR. Interestingly, an increase in AtTIP2;1-YFP signal observed in the pericycle, endodermis and new primordial cells located at the base of the developing LRP was correlated with the transient increase in *AtTIP2;1* mRNA measured by RT-qPCR.

LRP developmental process depends on the proper temporal and spatial expression of TIPs. Indeed, attempts to rescue the LRP emergence phenotype in the different mutated *tip* lines, by ectopic expression (using the 35S promoter) of *AtTIP* genes was not successful, except for a partial recovery in the triple *tip* mutant by AtTIP1;2. The full recovery of the LRP emergence phenotype was only obtained when *AtTIP2;1* was expressed under its endogenous promoter. As AtTIP2;1 is exclusively expressed in cells located at the base of developing LRPs, these data demonstrate an important role of AtTIP2;1 in these specific location possibly facilitating water movement from the stele to the LRP and the fast growth of these cells and/or the full LRP through the underlaying tissue. The exact role of AtTIP1;1 during LRP development remains vague, as single mutants were only slightly affected in LRP formation. AtTIP1;1 expression pattern remained rather constant throughout LRP development, except with a decrease in expression in the cortex cells facing the LRPs at late stages. In contrast, AtTIP1;2 abundance appears to be more tightly linked to LRP development. Its expression was indeed gradually modified with a higher expression in the stele tissues and a lower or no expression in the epidermis and cortex cells facing the developing LRP. Altogether, the AtTIP expression patterns suggest the presence of a gradient in AtTIP abundance and, therefore, in tonoplast water permeability between the LRP and its surrounding tissues (Fig. 10). This could contribute to the maintenance of a high turgor pressure in the cells at the base of the LRP by an influx of water from the stele and probably from the surrounding tissues, giving rise to cell growth, and a decrease in turgor pressure in

433 the overlaying cortex cells to allow LRP emergence. AtTIPs could also contribute to the
434 transcellular water flow from the vascular tissues to expanding cell territories of the LRPs.
435 These data highlight the importance of the cell type specificity and timing of *AtTIP*
436 expression and are in accordance with the results showing that disrupting cell water
437 permeability by ectopic expression of *AtPIP2;1* delayed LRP emergence in a WT background
438 (Peret et al., 2012).

439 While Peret et al. (2012) reported flattened LR primordial domes in the *Atpip2;1*
440 mutant, we observed only a small fraction of flattened LRPs in all of the analysed *tip* mutant
441 lines, the majority of them appearing normal even during early developmental stages.
442 Furthermore, Peret et al. (2012) did not report any change in root architecture in the *Atpip2;1*
443 mutant, as it was found for the triple *tip* mutant. It could be speculated that PIPs play a role in
444 mediating the water influx into the LRP structure whereas TIPs could be important during cell
445 expansion processes, in particular during late developmental stages after the LRP breaks the
446 casparian strip and rapidly emerges out of the root. This slightly differentiated functionality of
447 PIPs and TIPs during LRP emergence could account for the less pronounced occurrence of
448 flattened LRPs in the *tip* mutants compared to the *Atpip2;1* mutant (Peret et al., 2012), as well
449 as for the reduced number of LRs in the triple *tip* mutant.
450
451 **TIPs are not essential for elongation of the main root and the hypocotyl**

452 Single mutants for *tip1;1* and *tip1;2* as well as the *tip1;1* x *tip1;2* double mutant were
453 previously carefully analysed and no phenotype was observed with respect to macroscopic
454 appearance and water balance (Schussler et al., 2008; Beebo et al., 2009). In addition, *tip1;1*
455 mutant did not show any compensatory effect by an up-regulation of the expression of other
456 *AtTIP* genes (Schussler et al., 2008; Beebo et al., 2009), which is in agreement with the
457 present study. Under our growth conditions, we only observed a significant up-regulation of
458 *AtTIP2;1* in the *tip1;2* mutant compared to the wild-type which might partially compensate
459 for the loss of *AtTIP1;2*. However, in the *tip1;2* x *tip2;1* double- and *tip1;1* x *tip1;2* x *tip2;1*
460 triple mutant no such up-regulation of any *AtTIP* gene was detected. The absence of a clear
461 elongation defect of the main root of the triple *tip* mutant indicates a minor role of the
462 AtTIP1;1, AtTIP1;2 and AtTIP2;1 isoforms in this process. Since the tonoplast was shown to
463 be about 10 times more permeable to water than the plasma membrane (Maurel et al., 1997;
464 Niemietz and Tyerman, 1997), probably due to the high amount of TIPs in the tonoplast, it
465 remains to be determined why no more drastic phenotype was observed in the triple *tip*
466 mutant, where basically most of the TIP isoforms are absent. It could mean that the residual

467 water permeability of the tonoplast in these lines was sufficient to promote root elongation in
468 the tested conditions. It would be interesting to compare the water permeability of intact
469 vacuoles of the triple *tip* mutant and wild type plants by determining the swelling/shrinking
470 rates upon osmotic changes as described (Morillon and Lassalles, 1999).

471 Similarly to what was observed for the main roots, AtTIP1;1, AtTIP1;2 and AtTIP2;1
472 did not seem to play a major role during hypocotyl growth (Gendreau et al., 1997; Raz and
473 Koornneef, 2001). On the tissue level, the process of hypocotyl growth is very similar to root
474 elongation: various layers of cells elongate homogeneously in a single-dimensional manner.
475 The hypocotyls gain about 10 mm in length during 4 days in the dark, which is comparable to
476 that of the root. After 4 days under standard growth conditions, no difference of various *tip*
477 mutant lines compared to the wild-type was detected, except for the *tip1;1* mutant, which
478 exhibited slightly longer roots. These data were quite unexpected as the expression pattern of
479 *AtTIP* genes in Arabidopsis and other plant species suggested an important functional role of
480 these proteins in the main root and hypocotyl growths. The promoter of Arabidopsis *AtTIP1;1*
481 was shown to be active in the hypocotyl and root elongation zone (Ludevid et al., 1992).
482 Maize ZmTIP1;1 is highly expressed in expanding cells in roots and leaves (Barrieu et al.,
483 1998; Chaumont et al., 1998). An increased expression of TIPs is also observed in elongating
484 tissues of hypocotyls in soybean, castor bean and radish seedlings (Higuchi et al., 1998; Suga
485 et al., 2001; Eisenbarth and Weig, 2005). Once again, the basal water permeability of the
486 tonoplast in the Arabidopsis *tip* mutated lines could be sufficient to allow the generation and
487 maintenance of the turgescence essential for the cell elongation process under standard
488 growth conditions. Interestingly, we observed that increasing the medium osmolarity by
489 adding 400 mM mannitol resulted in a decrease of the main root length of the *tip* mutants
490 compared to wild-type plants (Fig. 3). In these conditions, higher tonoplast water permeability
491 would be required for the equilibrium of the cell water status during the cell growth process.
492

493 ## Materials and Methods

494 **Plant material and growth conditions**

495 The Arabidopsis *tip1;1* mutant is a T-DNA insertion mutant from the Salk Institute
496 collection (Alonso et al., 2003) and was obtained from the NASC stock center (seed stock
497 N519003). The Arabidopsis *tip1;2* and *tip2;1* mutants were previously identified in the SLAT
498 collection (Tissier et al., 1999) using the Sequenced Insertion Site (SINS) database, and seed
499 stocks (N116827, N118785) were obtained from the NASC stock center. The *tip1;2* and

tip2;1 mutants display a defective Suppressor-mutator (dSpm) insertion within the first and second exons, respectively (Supplemental Fig. 1). Quantitative real-time PCR (RT-qPCR) experiments showed that *AtTIP1;2* and *AtTIP2;1* mRNA levels were reduced to less than 3% in *tip1;2* and *tip2;1* mutant, respectively, compared to the level in wild-type plants (data not shown). In order to obtain a *tip1;2* x *tip2;1* double mutant line, the F2 progeny of a cross between the two mutant lines was PCR-screened to identify plants with a recombinant chromosome bearing the two mutations using the *AtTIP*-specific primers TIP12F-652 and TIP12UTR3R371 or TIP21F-683 and TIP21UTR3R371 for *AtTIP1;2* or *AtTIP2;1*, respectively, along with the transposon-specific primer dSpm1 to amplify wild-type and mutant alleles (Supplemental Table 1). A plant homozygous for the *tip2;1* mutation and heterozygous for the *tip1;2* mutation was identified and then allowed to self-pollinate. Plants homozygous for both mutations were identified in the offspring by PCR. Reduction in *AtTIP* mRNA levels was checked by RT-qPCR in the next generation (data not shown).

The *tip1;1* x *tip1;2* x *tip2;1* triple mutant was generated by crossing homozygote *tip1;1* x *tip1;2* and *tip1;1* x *tip2;1* double mutants, which were generated from the insertion line SM_3_32402 (*tip1;1*) and GABI_880H12 (*tip1;2*) (Schussler et al., 2008), and SM_3_32402 (*tip1;1*) and SM_3_38811 (*tip2;1*) by floral crossing. The *tip2;1* insertion mutant was kindly supplied by N. von Wirén (University of Hohenheim, Stuttgart, Germany) and originated from the Nottingham Arabidopsis Stock Centre (NASC, http://arabidopsis.info). Homozygote insertion was verified by PCR using the primers TIP21F132 and TIP21R395 in order to amplify the genomic sequence of the wild type *AtTIP2;1* and the primers dSpm1 and TIP21R729 to verify the transposon insertion (Supplemental Table 1).

The Arabidopsis line expressing AtTIP2;1 fused to yellow fluorescent protein (YFP) under the control of the endogenous *AtTIP2;1* promoter (~1,2 kb) was described in (Gattolin et al., 2009). Arabidopsis wild-type Columbia (Col-0) and *tip* mutants seeds were surface sterilized in 3% (v/v) commercial bleach and rinsed five times with sterile distilled water. All seeds were placed on 60 ml ½ Murashige and Skoog medium (MS) at pH 5.8, solidified with 0.85 % (w/v) agar in squared plates (ca. 120 × 120 mm). The seeds were stratified for 2 to 4 days at 4°C to obtain homogenous germination. For phenotyping and expression analysis, the medium was supplemented by 1.5 % sucrose and plants were grown at 60 µmol photons m^{-2} sec^{-1} under long day conditions (16 h light/8 h dark). For LRE experiments, plants were grown without the addition of sucrose at 150 µmol photons m^{-2} sec^{-1} under long day conditions.

Plasmid constructions and plant transformation

The cDNAs of *AtTIP1;1*, *AtTIP1;2* and *AtTIP2;1* were amplified by PCR (for primers see Supplemental Table 3) from single strand cDNA. PCR fragments were cloned using an uracil excision-based improved high-throughput USER cloning technique into the USER-compatible vector pCambia2300 35S u (Nour-Eldin et al., 2006). The constructs were verified by sequencing. To obtain *AtTIP1;2::AtTIP1;2-GFP* and *AtTIP2;1::AtTIP2;1-GFP* constructs, the genomic sequences of *AtTIP1;2* and *AtTIP2;1* starting ~3kb upstream of the translational start codon and ending before the stop codon were amplified by PCR (for primers see Supplemental Table 3), cloned in the gateway entry vector pDONR221 (Invitrogen) and transferred using LR recombination in front of the *GFP* in the modified pMDC83 binary destination vector (Curtis and Grossniklaus, 2003) in which the double 35S promoter was deleted. The genomic sequence of *AtTIP2;1* (including the ~3kb promoter region) inserted in pDONR221 was recombined into the pGWB1 vector (Nakagawa et al., 2007) to create an untagged construct used to complement the triple *tip* mutant line. The binary vectors were introduced into *Agrobacterium tumefaciens* strain GV3101 by electroporation and recombinant *Agrobacterium* lines were used to transform Arabidopsis plants through the floral dip method (Clough and Bent, 1998). Transgenic plants were selected on half-strength MS agar plates containing kanamycin (50 mg/l).

RT-qPCR

Total RNA was extracted from roots and shoots of 12 day old seedlings using RNeasy RNA plant extraction mini kit (Qiagen, Maryland, USA) and chromosomal DNA was digested on the column during the RNA isolation process using DNase I (Qiagen, Maryland, USA), according to manufacturer's recommendation. RNA was quantified by spectrophotometry at 260 nm. The RNA quality was checked on agarose gel. One µg of total RNA was transcribed into cDNA with oligo(dT) primers for 1 h at 42°C with M-MuLV Reverse Transcriptase (Promega, Madison, USA) followed by 5 min at 85°C in a thermo cycler as described previously (Hachez et al., 2006). Primer pairs were described by (Alexandersson et al., 2005) or designed using Quantprime (www.quantprime.de (Arvidsson et al., 2008)) (Supplemental Table 2). RT-qPCR was performed using 1 µl of 1:10 diluted cDNA samples in a 25 µl reaction volume containing 300 nM gene-specific primers and 12.5 µl SYBR Green 1 PCR Mix (Eurogentec, Liege, Belgium) in a StepOnePlus thermocycler (Applied Biosystems, Foster City, CA) with the following program: (i) 50°C for 2 min, (ii)

95°C for 10 min, (iii) 95°C for 15 sec, (iv) 60°C for 30 sec, (iii-iv for 40 cycles). No template controls were included in the assay and the absence of genomic DNA was verified by PCR using primers targeting an intronic region of the control gene *MADS AFFECTING FLOWERING 5* (MAF5, At5g65080, Supplemental Table 2). Melting curve analyses were performed for all samples by elevating the temperature from 55°C to 95°C. Normalization was performed using geometric averaging of three control genes: actin, α-tubulin, and ubiquitin (Bustin et al., 2009).

Growth measurements

Six or four seedlings of two or three genotypes, respectively, were grown per plate, resulting in twelve seedlings per plate. Genotypes were spatially randomized and each genotype appeared on at least three plates. For root growth experiment, the position of the root tips was marked once per day using a razor blade. At the end of the experiments, the plates were scanned and root lengths were measured on the images assuming straight lines between the root base and marks of the Petri dish using ImageJ.

Root bending assay

Five-day old seedlings grown on vertical ½ MS plates were subjected to a gravitropic stimulus by a 90º turn. As it was previously reported that lateral root formation is affected by the uptake of sucrose from the medium (Macgregor et al., 2008), plants were grown without sucrose. Seedlings were harvested 18 and 42 h post gravitropic induction (pgi) of lateral root formation, the tissue was cleared, and lateral root primordia (LRP) stages at the bending site were recorded (Malamy and Benfey, 1997).

Tissue clearing and microscopy analysis

For LRP observation, root tissues were cleared using acidified methanol (7:2:1 H_2O:methanol:acetic acid) for 20 min at 55°C followed by a basic ethanol (7 % NaOH, 60 % ethanol) treatment for 15 min at room temperature. The tissue was rehydrated by an ethanol series of 40 %, 20 % and 10 % for 15 min for each concentration at room temperature. For storage and observation, roots were kept in 50 % glycerol. Seedlings, immersed in 50 % glycerol, were placed on microscope slides and the developmental stage of the LRP was rated using standard light microscope with 20x or 40x objective (Leica DMR, Wetzlar, Germany). The expression of fluorescent-tagged AtTIPs under the control of their endogenous promoter was observed in non-treated roots using a confocal microscope (Zeiss LSM710). YFP was

excited at 514 nm and the fluorescence signal was recorded in the range from 524 to 580 nm; GFP was excited at 488 nm and the signal was detected from 499 to 553 nm. Propidium iodide (PI) was excited using the laser according to the fluorescent protein observed (488 or 514 nm for GFP or YFP, respectively) and the signal was detected in the range from 596 to 710 nm.

Statistical analysis

The Student's *t*-test was applied in order to determine the significance of differences of average values between wild-type and mutant lines. For statistical analysis of the developmental stage distribution of LRPs, we applied the Pearson's independency test on standard contingency tables for sequential pairwise comparisons (Zar, 2010) of the developmental stage distribution of LRPs between relevant genetic backgrounds.

Acknowledgements

We thank the imaging platform IMABIOL.

Figure legends

Figure 1. Expression levels of *AtTIP* mRNAs in Arabidopsis wild-type and *tip* mutant lines. *AtTIP* mRNA levels in leaves (A) and roots (B) of 12 day-old Arabidopsis grown on vertical plates containing 1/2 MS medium, determined by RT-qPCR. The ten *AtTIP* isoforms where tested in the assay. Only the detected isoforms are shown. Data is given as means +/- SD. *Double*: *tip1;2 x tip2;1* double mutant; *triple*: *tip1;1 x tip1;2 x tip2;1* triple mutant.

Figure 2. Root growth of Arabidopsis *tip* mutants under normal conditions and osmotic stress. A, Root length of Arabidopsis wild-type (WT) and *tip* mutant lines over time grown on vertical plates containing 1/2 MS medium supplemented with 1.5 % sucrose. Data is given as means of 48-72 plants +/- SE. B, Root length of Arabidopsis *tip* mutant lines over time after transferring seven day-old seedlings from (A) to vertical plates containing 1/2 MS medium in the presence or absence of 1.5 % sucrose supplemented with 0, 200 or 400 mM mannitol.

Data is given as means of 6-16 plants +/- SE. Stars indicate significant differences from the wild-type (t-test, p-value < 0.05).

Figure 3. The Arabidopsis *tip1;1 x tip1;2 x tip2;1* triple mutant shows a reduced number of lateral roots. A, Arabidopsis wild-type (WT) and *tip1;1 x tip1;2 x tip2;1* triple mutant (*triple*) where grown vertically for twelve days on 1/2 MS medium supplemented with 1.5 % sucrose; bar = 10 mm. B, Compared to wild-type, the triple *tip* mutant exhibits slightly shorter main roots. C, Compared to wild-type, the triple *tip* mutant exhibits a strong decrease in the number of lateral roots. Means are given +/- SE, n = 47 plants. Stars indicate significant differences from wild-type (t-test, $p < 0.05$). D, Length distribution of all lateral roots from both, 50 wild-type and *tip1;1 x tip1;2 x tip2;1* triple *tip* mutant plants (n = 381 and 288 for WT and *triple*, respectively).

Figure 4. Disrupted *AtTIP* expression causes delayed LRP development. A, To synchronise lateral root development, plants were subjected to a 90° gravitropic stimulus. B and C, Lateral root primordia stages (from 0 to VIII, Em: emerged; (Malamy and Benfey, 1997)) are expressed in percentage of the total number of LRPs, 18 h (B) and 42 h (C) pgi. Double: *tip1;2 x tip2;1*, triple: *tip1;1 x tip1;2 x tip2;1*. n = 12 –24, pooled from two independent experiments. Statistical analysis was performed using standard contingency tables to sequentially compare the lines with each other (see Materials and Methods).

Figure 5: Expression of AtTIP1;1 and AtTIP1;2 during lateral root development. Seven to eight day-old roots from *AtTIP1;1::AtTIP1;1-GFP* (A-H) and *AtTIP1;2::AtTIP1;2-GFP* (I-P) transgenic seedling were stained with propidium iodide for 5 min and lateral root at different developmental stages were visualised by confocal laser scanning microscopy. A-D and I-L, Single optical sections of the transmitted light signal showing the developmental state of the lateral root. E-H and M-P, Maximal projections of optical z-stacks of merged signals from GFP (green) and propidium iodide fluorescence (red). The dome shape of the

LRP is indicated by dotted lines at the developmental stages II, IV and VI (Malamy and Benfey, 1997). Scale bars: 20 µm.

Figure 6: Expression of AtTIP2;1 during LRP development. A, *AtTIP2;1* expression level was followed after gravitropic induction of lateral root formation and dissection of the root bend. Expression level is shown as a function of pgi relative to the expression right after the gravitropic induction. Approximated LRP developmental stages (Malamy and Benfey, 1997) at the individual time pgi are indicated. Data are presented as means of two biological replications +/- SD. B-L, Roots from *AtTIP2;1::AtTIP2;1-YFP* plants (Gattolin et al., 2009) were stained with propidium iodide for 5 min, and LRPs at different developmental stages were investigated by confocal laser scanning microscopy. B and F, LRP stage II, approximately corresponding to the developmental status at about 18 h pgi. C and G, LRP stage IV, approximately corresponding to 24 h pgi. D and H, LRP stage VI, approximately corresponding to 36 h pgi. E and I, LRP stage VII, approximately corresponding to 42 h pgi. B-E, Single optical sections of the transmitted light signal showing the developmental state of the LRP. F-I, Maximal projections of optical z-stacks of merged signals from YFP (yellow) and propidium iodide fluorescence (red). The dome shape of the LRP is indicated by dotted lines. J-L, Magnification of the AtTIP2:1-YFP expressing cells during LRP stage IV, IV and VIII. The arrows indicate triangular shaped cells containing intense AtTIP2;1-YFP signal. The images show representative results for each LRP stage. Scale bars: 50 µm.

Figure 7. **Orthogonal sections of a LRP in the developmental stage IV and VI.** A, Orientation of the space dimensions during confocal imaging. The cylinder represents a root section, which is imaged in several XY planes with different focus depth Z. This so called z stack can be cut along XZ or YZ planes allowing virtual tissue sectioning. B-H, AtTIP2;1-YFP in a stage IV LRP (from Fig 7. C, G, J). B, XY plane, the lines indicate the positions of the according YZ planes shown in C-H. The scheme in C illustrates the various root cell types in the cross section: “C” denotes cortex cells, “E” denotes endodermis cells. The arrow points toward the AtTIP2;1-YFP signal, located in newly created LRP cells adjacent to the endodermis. I-O, AtTIP2;1-YFP in a stage VI LRP (from Fig. 7. E, I, L). I, XY plane, the lines indicate the according positions of the YZ planes shown in J-O. The scheme in J

illustrates the positions of cortex cells. The YFP signal is located underneath the cortex cells in the newly developed primordial cells as well as in the neighbouring endodermis cells.

Figure 8. Constitutive expression of *AtTIP* genes in the *tip* mutant lines alters LRP development. A, Transgene *AtTIP* expression in the complemented *tip* mutant lines determined by RT-qPCR and compared to wild-type control. *Double*: *tip1;2* x *tip2;1*, *triple*: *tip1;1* x *tip1;2* x *tip2;1*. "*C*" indicates that the line is complemented, followed by the number of the *AtTIP* isoform and the number of the independently selected line. E.g. "*triple C1;2#21*" represents the *tip1;1* x *tip1;2* x *tip2;1* mutant complemented with *AtTIP1;2*, selected line no.21. B, Developmental stage distribution (from 2 to 8, Em: emerged; (Malamy and Benfey, 1997)) of LRP 42 h pgi in Arabidopsis *tip* mutant and the complemented lines. n = 23 - 102, pooled from two independent experiments. Statistical analysis was performed using standard contingency tables to sequentially compare relevant lines (see Materials and Methods). Only lines corresponding to one mutant line (grouped by horizontal lines in the chart) where compared with each other and the wild-type.

Figure 9. Expression of *AtTIP2;1* under the control of its own promoter rescues the LRE phenotype of the triple *tip* mutant. Developmental stage distribution (from III to VIII, Em: emerged; (Malamy and Benfey, 1997)) of LRP 42 h pgi from seedlings of wild type (WT), the *tip1;1 x tip1;2 x tip2;1* triple mutant (triple), transformed triple tip mutant with *p(promoter)TIP2;1::TIP2;1* or *pTIP2;1::TIP2;1:GFP* fusions lines. n = 22 – 38. Statistical analysis was performed using standard contingency tables to sequentially compare relevant lines (see Materials and Methods).

Figure 10. A tightly regulated TIP expression pattern is required for fast LRP development. After the LRP development is initialized, a gradient of TIP1;2 expression (red; dark: high expression, light: low expression) is observed from inner to outer root tissues and down-regulated in cortex cells facing the initialized LRP. At the same time, TIP2;1 expression (green) is up-regulated in cells located at the base of the LRP. This could result in a gradient in vacuolar water permeability between the base of the LRP on one side and the LRP

surrounding tissues on the other side. The cells at the base of the LRP therefore could expand rapidly and allow the fast growth and emergence of the LRP throughout the overlaying tissues.

.

Supplemental information

Supplemental Table 1. Primers used to create multiple *tip* mutant lines and verify the obtained lines

Gene	Primer name	Primer sequence
AtTIP1;2	TIP12F-652	5'- CCGAAAAAGTTACCAGCCCAT -3'
	TIP12UTR3R 371	5'-AAAAACGGAAATGAAAACCAAAAA-3'
AtTIP2;1	TIP21F-683	5'-AATCACGTTAAACCGGCCATATTACTTA-3'
	TIP21F132	5'-GCTGACGTCGGACGCTGC-3'
	TIP21R395	5'- GAAATCAGCAGAAGCAAGAGGA-3'
	TIP21R729	5'-GAAATCAGCAGAAGCAAGAGGA-3'
	TIP21UTR3R 371	5'-ATAGGTTGTCATACAACAATTGCCAGAGT-3'
Transposon	dSpm1	5'-CTTATTTCAGTAAGAGTGTGGGGTTTTGG-3'

Supplemental Table 2. Primers used for RT-qPCR to determine the expression level of all *TIP* isoforms in the *tip* mutant lines and wild-type.

Gene name	Primer name	Primer sequence	Ref.
AtTIP1;1	TIP11F129	5'-CGGCGTTGGCTGAGTTCATTTC-3'	
	TIP11R195	5'-AAAGCCATGCCAGAGCCTGAAC-3'	QP
AtTIP1;2	TIP12F458	5'-TCGCCGCTTGTTTCCTCCTTAG-3'	QP
	TIP12R520	5'-AGAGACCGAACGCTGGAATTGG-3'	
AtTIP1;3	TIP13F517	5'-TCATTGCGCCTTTGGCGATTGG-3'	QP
	TIP13R594	5'-TCATCGATGCACCGTCGAAAGC-3'	
AtTIP2;1	TIP21F114	5'-TGCCATTGCCTACGCAAAGCTGAC-3'	A
	TIP21R211	5'-CGGCCACGAAGAGAGCAAAACCAT-3'	
AtTIP2;2	TIP22F370	5'-AATGGCGAGAGCGTACCGACTCAT-3'	A
	TIP22R519	5'-AGCAATGGTCCCGAGTGAACCTTT-3'	

AtTIP2;3	TIP23F358 TIP23R426	5'-TCAGTGTCTTGGCTCCATCGTC-3' 5'-GTCGGTACGCTCTTGCCATTAG-3'	QP
AtTIP3;1	TIP31F599 TIP31R668	5'-GGCTCACAACAAACGGCATGAG-3' 5'-AGTCCATTAACCGCTCCAACACC-3'	QP
AtTIP3;2	TIP32F123 TIP32R222	5'-AGGCTCAATCCTCGCTCTAGACAA-3' 5'-TGCATGAGCTAACGCCACCAGA-3'	A
AtTIP4;1	TIP41F323 TIP41R369	5'-CCACATCAGCGTATTCCGTGCATT-3' 5'-TCCCATTCCTCCGGTGAGGTAACT-3'	A
AtTIP5;1	TIP51F398 TIP51R466	5'-AAAGTAACCGTCATGGAACAGCAC-3' 5'-TGCTCCAAATCCAGTCATTTCTCC-3'	QP
ACT1	ActinF ActinR	5'-TGGAACTGGAATGGTTAAGGC-3' 5'-TCTCCAGAGTCGAGCACAATA-3'	S
TUA4	a-Tubulin a-Tubulin	5'-GGTCACCACCTGGAACAACT-3' 5'-TGGCACCATCAAGACAAGACAAAGA-3'	S
UBQ10	UbiquitinF UbiquitinR	5'-CACACTCCACTTGGTCTTGCGT-3' 5'-TGGTCTTTCCGGTGAGAGTCTTCA-3'	L
MAF5	MAF5F MAF5R	5'-TTTTTTGCCCCCTTCGAATC-3' 5'-ATCTTCCGCCACCACATTGTAC-3'	C

The numbers refer to the position of the nucleotide sequence compared to the ATG start codon. A: Alexandersson *et al*. (2005) C: Czechowski *et al*. (2005); L: Li *et al*. (2006); QP: Quantprime (Arvidsson *et al.*, 2008); S: Schussler *et al.* (2008).

Supplemental Table 3. Primers used for cloning.

Gene	Primer name	Primer sequence
AtTIP1;1	U-TIP11	5'-*GGCTTAAU*ATGCCGATCAGAAACATC-3'
	TIP11-U	5'-*GGTTTAAU*TCAGTAGTCTGTGGTTGG-3'
AtTIP1;2	U-TIP12	5'-*GGCTTAAU*ATGCCGACCAGAAACATC-3'
	TIP12-U	5'-*GGTTTAAU*TCAGTAATCGGTGGTAGG-3'
AtTIP2;1	U-TIP21	5'-*GGCTTAAU*ATGGCTGGAGTTGCCTTT-3'
	TIP21-U	5'-*GGTTTAAU*TTAGAAATCAGCAGAAGC-3'
YFP	U-YFP	5'-*GGCTTAAU*ATGGTGAGCAAGGGCGAG-3'
	UBOX-U	5'-*GGTTTAAU*TAAGGAATCCTTAATTAAGC-3'
gAtTIP1;2	attB1-S1	5'-GGGGACAAGTTTGTACAAAAAAGCAGCAGGCTTCTTCAGTCGCTGTGTCCA-3'
	attB2-S1	5'-GGGGACAAGTTTGTACAAAAAAGCTGGGTACCAGTAATCGGTGGTAGGCAAT-3'

gAtTIP2;1	attB1-D1	5'-GGGGACAAGTTTGTACAAAAAAGCAGGCTTCG AGAAAGATGCAAAGCAAA
	attB2-D1	5'-GGGGACAAGTTTGTACAAAAAAGCTGGGTAGA AATCAGCAGAAGCAAGAGGA

739

740 The sequences for the formation of the "sticky ends" during USER cloning are indicated in
741 *italics*. *g* indicates that the primers were used to clone the genomic DNA (starting ~3kb
742 upstream sequence of the translational start codon and ending before the stop codon)

743

744 **Supplemental Figure 1. Verification of the homozygosity of the insertion in the different**
745 ***tip* mutant lines.** Numbers in red and black indicate the position on the cDNA and the
746 genomic DNA, respectively (position 1 starting at the start codon). Numbers on the primers
747 refer to the cDNA positions. A, Insertion in the *tip1;1* single mutant. The T-DNA insertion
748 induced the loss of 13 bp within the 5' non-coding region. B, Insertion in the *AtTIP1;2* gene
749 of *tip1;2* single and *tip1;2 x tip2;1* double mutant. C, Insertion in the *AtTIP2;1* gene of *tip2;*1
750 single and *tip1;2 x tip2;1* double mutant. D, Insertions in the *tip1;1 x tip1;2 x tip2;1* triple
751 mutant. The left panels show the PCR analyses performed from the genomic DNA of the
752 different wild-type and mutant lines using the indicated primers.

753

754 **Supplemental Figure 2. Independent *tip* mutants exhibit delay in LRP development.** A,
755 Verification of the dSpm or T-DNA insertions in the second, independent batch of *tip* mutants:
756 *tip1;1-2*, *tip1;2-2* (Schussler et al., 2008) and *tip2;1-2* (Schüssler and Schjoerring,
757 unpublished data) by PCR using the primers given in Table1, according to the scheme shown
758 in Figure 1. B, Developmental stage distribution (Developmental stage distribution (from III
759 to VIII, Em: emerged; (Malamy and Benfey, 1997)) of LRP 42 h pgi. n = 20 – 77.Statistical
760 analysis was performed using standard contingency tables to sequentially compare relevant
761 lines (see Materials and Methods).

762

763

764

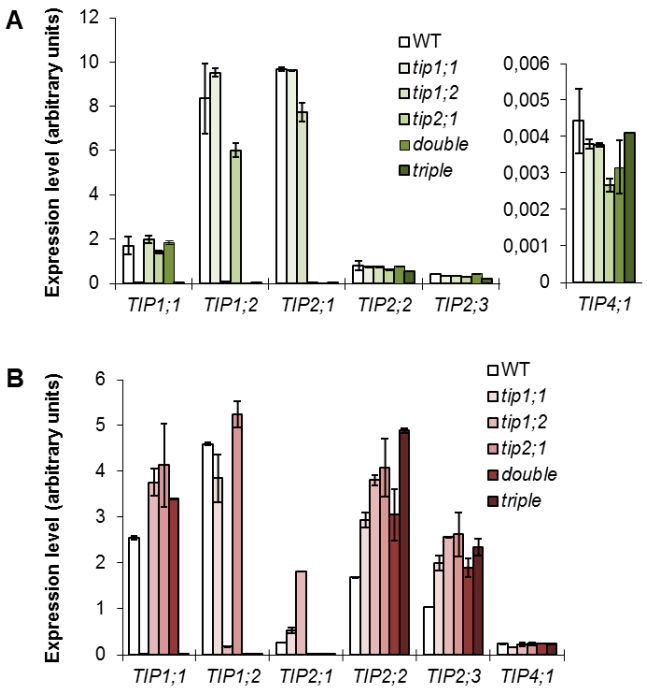

Figure 1. Expression levels of *AtTIP* mRNAs in Arabidopsis wild-type and *tip* mutant lines. *AtTIP* mRNA levels in leaves (A) and roots (B) of 12 day-old Arabidopsis grown on vertical plates containing 1/2 MS medium, determined by RT-qPCR. The ten *AtTIP* isoforms where tested in the assay. Only the detected isoforms are shown. Data is given as means +/- SD. *Double*: *tip1;2 x tip2;1* double mutant; *triple*: *tip1;1 x tip1;2 x tip2;1* triple mutant.

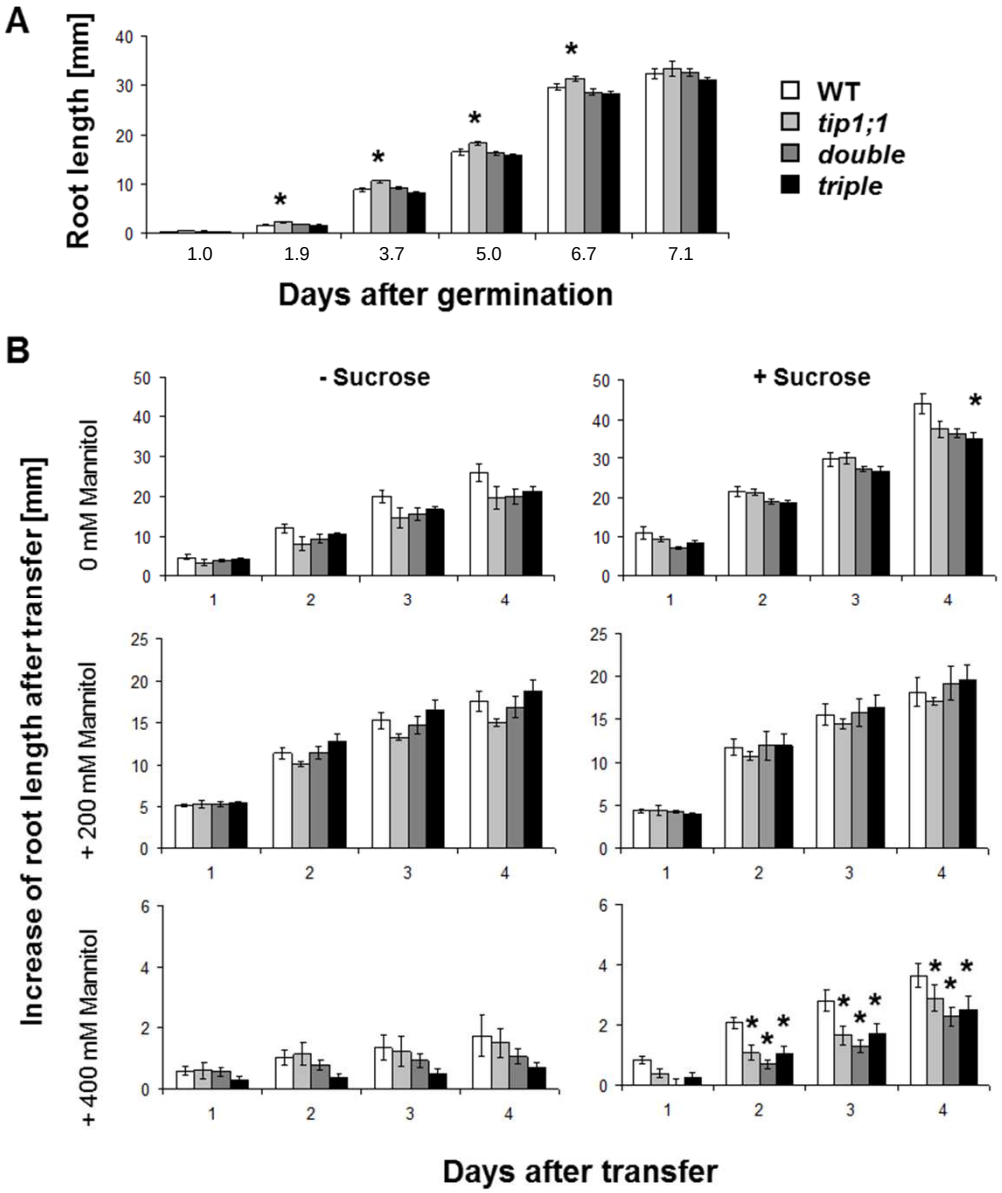

Figure 2. Root growth of Arabidopsis *tip* mutants under normal conditions and osmotic stress. A, Root length of Arabidopsis wild-type (WT) and *tip* mutant lines over time grown on vertical plates containing 1/2 MS medium supplemented with 1.5 % sucrose. Data is given as means of 48-72 plants +/- SE. B, Root length of Arabidopsis *tip* mutant lines over time after transferring seven day-old seedlings from (A) to vertical plates containing 1/2 MS medium in the presence or absence of 1.5 % sucrose supplemented with 0, 200 or 400 mM mannitol. Data is given as means of 6-16 plants +/- SE. Stars indicate significant differences from the wild-type (t-test, p-value < 0.05).

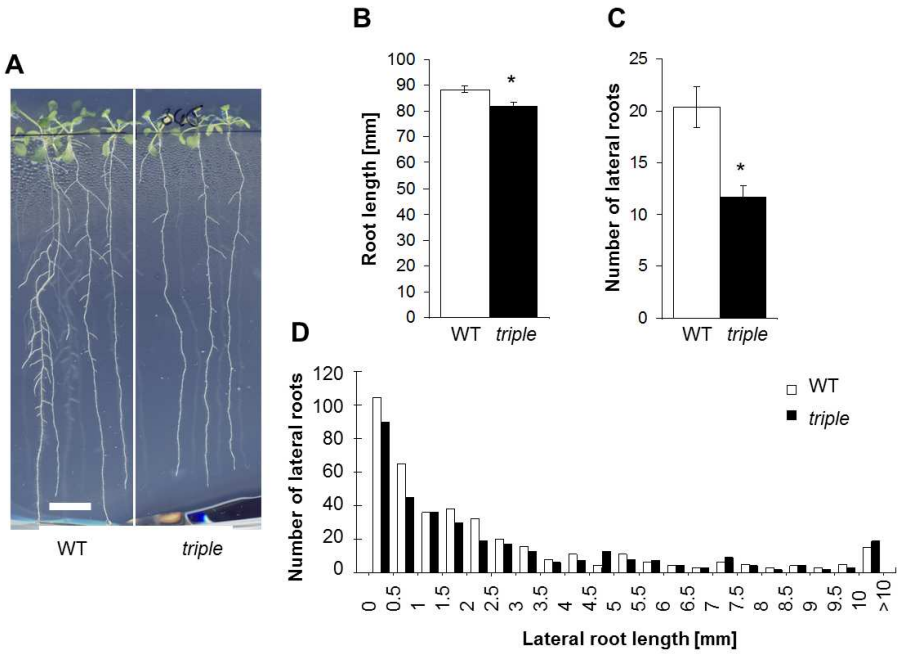

Figure 3. The Arabidopsis *tip1;1 x tip1;2 x tip2;1* triple mutant shows a reduced number of lateral roots. A, Arabidopsis wild-type (WT) and *tip1;1 x tip1;2 x tip2;1* triple mutant (*triple*) where grown vertically for twelve days on 1/2 MS medium supplemented with 1.5 % sucrose; bar = 10 mm. B, Compared to wild-type, the triple *tip* mutant exhibits slightly shorter main roots. C, Compared to wild-type, the triple *tip* mutant exhibits a strong decrease in the number of lateral roots. Means are given +/- SE, n = 47 plants. Stars indicate significant differences from wild-type (t-test, $p < 0.05$). D, Length distribution of all lateral roots from both, 50 wild-type and *tip1;1 x tip1;2 x tip2;1* triple *tip* mutant plants (n = 381 and 288 for WT and *triple*, respectively).

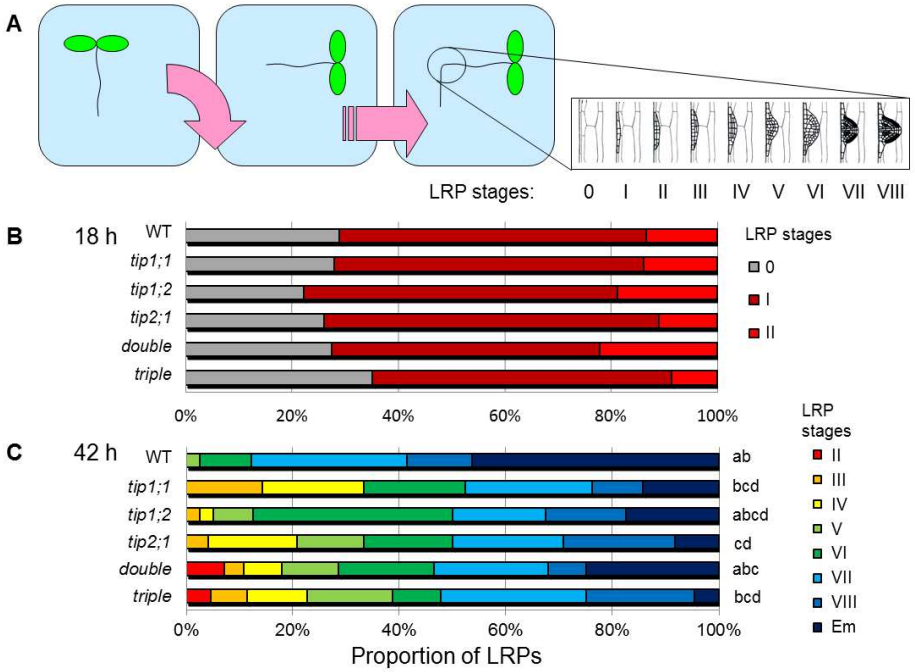

Figure 4. Disrupted *AtTIP* expression causes delayed LRP development. A, To synchronise lateral root development, plants were subjected to a 90° gravitropic stimulus. B and C, Lateral root primordia stages (from 0 to VIII, Em: emerged; (Malamy and Benfey, 1997)) are expressed in percentage of the total number of LRPs, 18 h (B) and 42 h (C) pgi. Double: *tip1;2 x tip2;1*, triple: *tip1;1 x tip1;2 x tip2;1*. n = 12 –24, pooled from two independent experiments. Statistical analysis was performed using standard contingency tables to sequentially compare the lines with each other (see Materials and Methods).

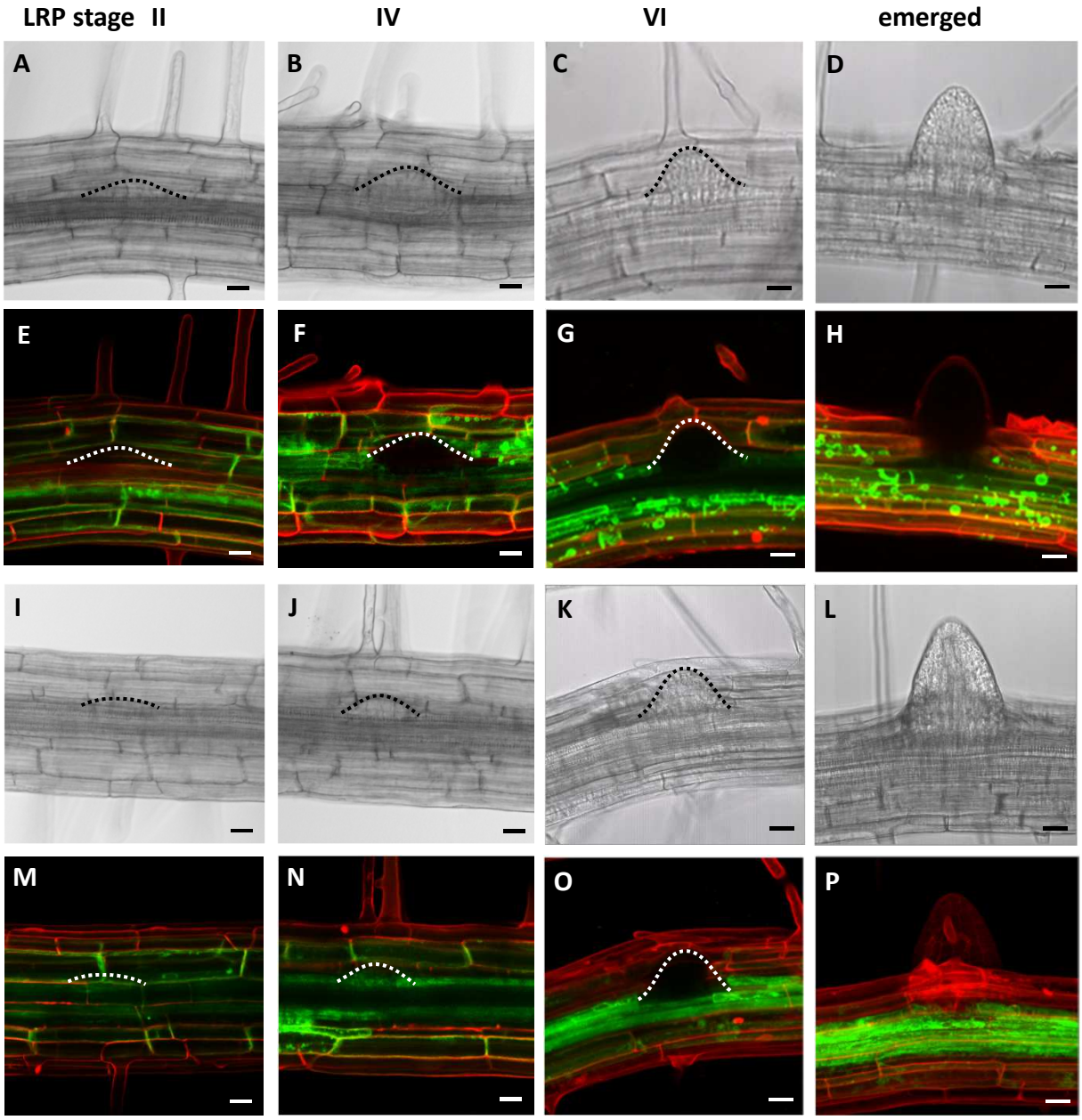

Figure 5. Expression of AtTIP1;1 and AtTIP1;2 during lateral root development. Seven to eight day-old roots from *AtTIP1;1::AtTIP1;1-GFP* (A-H) and *AtTIP1;2::AtTIP1;2-GFP* (I-P) transgenic seedling were stained with propidium iodide for 5 min and lateral root at different developmental stages were visualised by confocal laser scanning microscopy. A-D and I-L, Single optical sections of the transmitted light signal showing the developmental state of the lateral root. E-H and M-P, Maximal projections of optical z-stacks of merged signals from GFP (green) and propidium iodide fluorescence (red). The dome shape of the LRP is indicated by dotted lines at the developmental stages II, IV and VI (Malamy and Benfey, 1997). Scale bars: 20 µm.

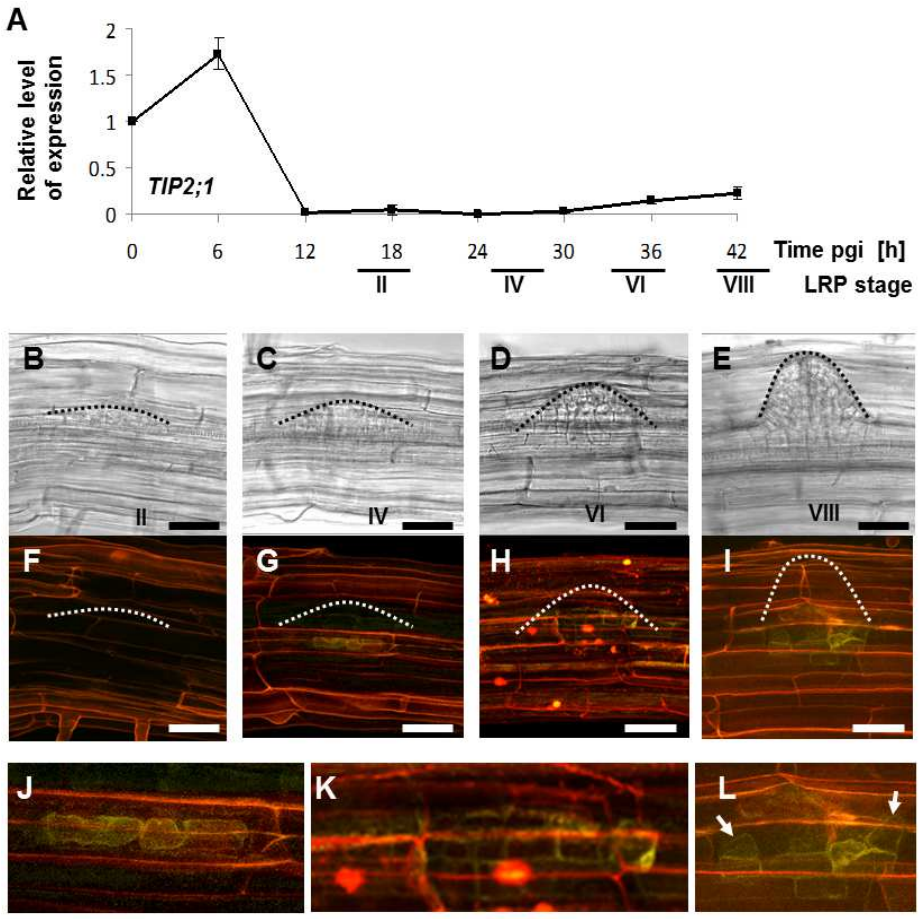

Figure 6. Expression of AtTIP2;1 during LRP development. A, AtTIP2;1 expression level was followed after gravitropic induction of lateral root formation and dissection of the root bend. Expression level is shown as a function of pgi relative to the expression right after the gravitropic induction. Approximated LRP developmental stages (Malamy and Benfey, 1997) at the individual time pgi are indicated. Data are presented as means of two biological replications +/- SD. B-L, Roots from AtTIP2;1::AtTIP2;1 YFP plants (Gattolin et al., 2009) were stained with propidium iodide for 5 min, and LRPs at different developmental stages were investigated by confocal laser scanning microscopy. B and F, LRP stage II, approximately corresponding to the developmental status at about 18 h pgi. C and G, LRP stage IV, approximately corresponding to 24 h pgi. D and H, LRP stage VI, approximately corresponding to 36 h pgi. E and I, LRP stage VII, approximately corresponding to 42 h pgi. B-E, Single optical sections of the transmitted light signal showing the developmental state of the LRP. F-I, Maximal projections of optical z-stacks of merged signals from YFP (yellow) and propidium iodide fluorescence (red). The dome shape of the LRP is indicated by dotted lines. J-L, Magnification of the AtTIP2:1 YFP expressing cells during LRP stage IV, IV and VIII. The arrows indicate triangular shaped cells containing intense AtTIP2;1-YFP signal. The images show representative results for each LRP stage. Scale bars: 50 µm.

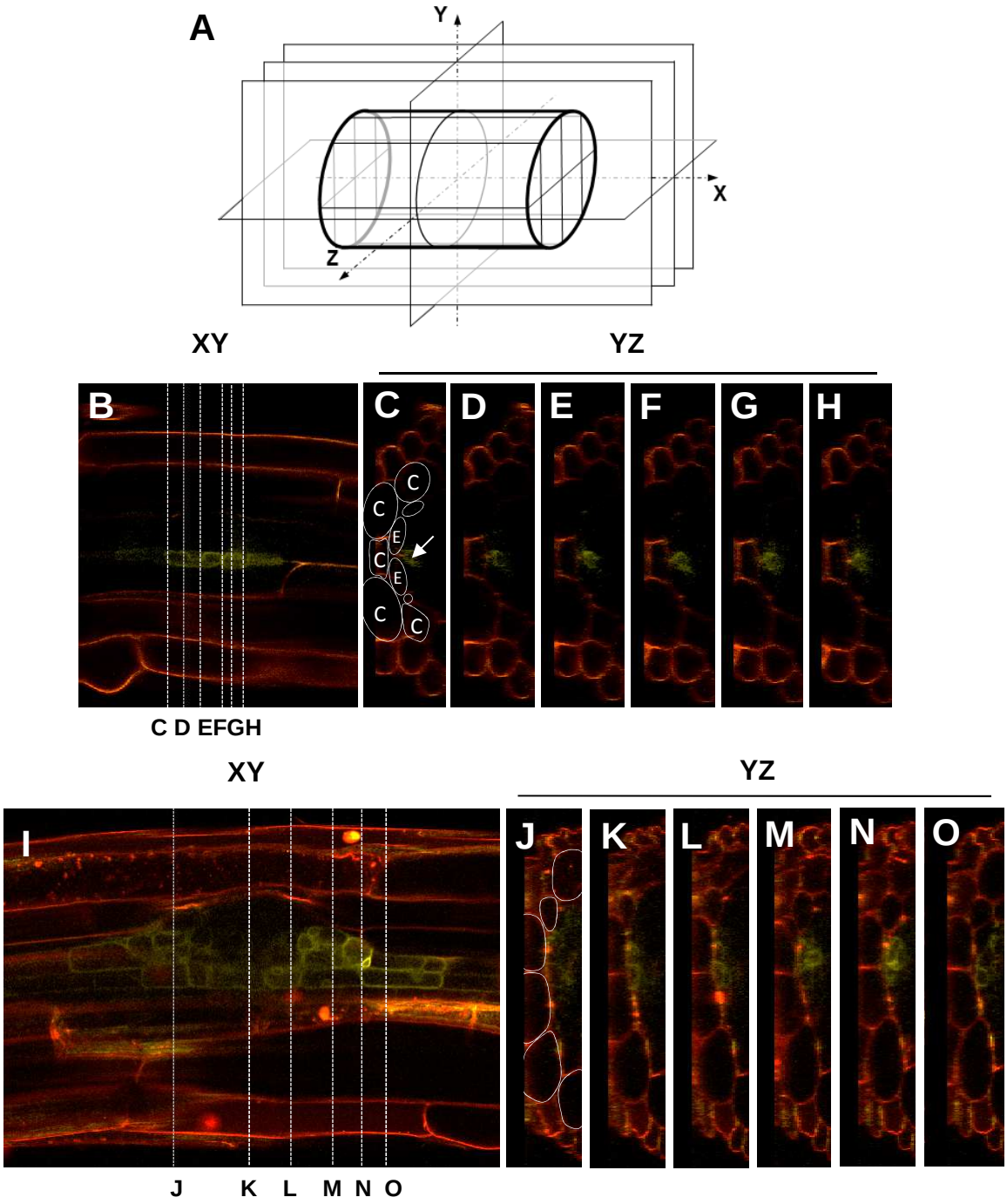

Figure 7. Orthogonal sections of LRPs in the developmental stages IV and VI. A, Orientation of the space dimensions during confocal imaging. The cylinder represents a root section, which is imaged in several XY planes with different focus depth Z. This so called z stack can be cut along XZ or YZ planes allowing virtual tissue sectioning. B-H, AtTIP2;1-YFP in a stage IV LRP. B, XY plane, the lines indicate the positions of the according YZ planes shown in C-H. The scheme in C illustrates the various root cell types in the cross section: “C” denotes cortex cells, “E” denotes endodermis cells. The arrow points toward the AtTIP2;1-YFP signal, located in newly created LRP cells adjacent to the endodermis. I-O, AtTIP2;1-YFP in a stage VI LRP. I, XY plane, the lines indicate the according positions of the YZ planes shown in J-O. The scheme in J illustrates the positions of cortex cells. The YFP signal is located underneath the cortex cells in the newly developed primordial cells as well as in the neighbouring endodermis cells.

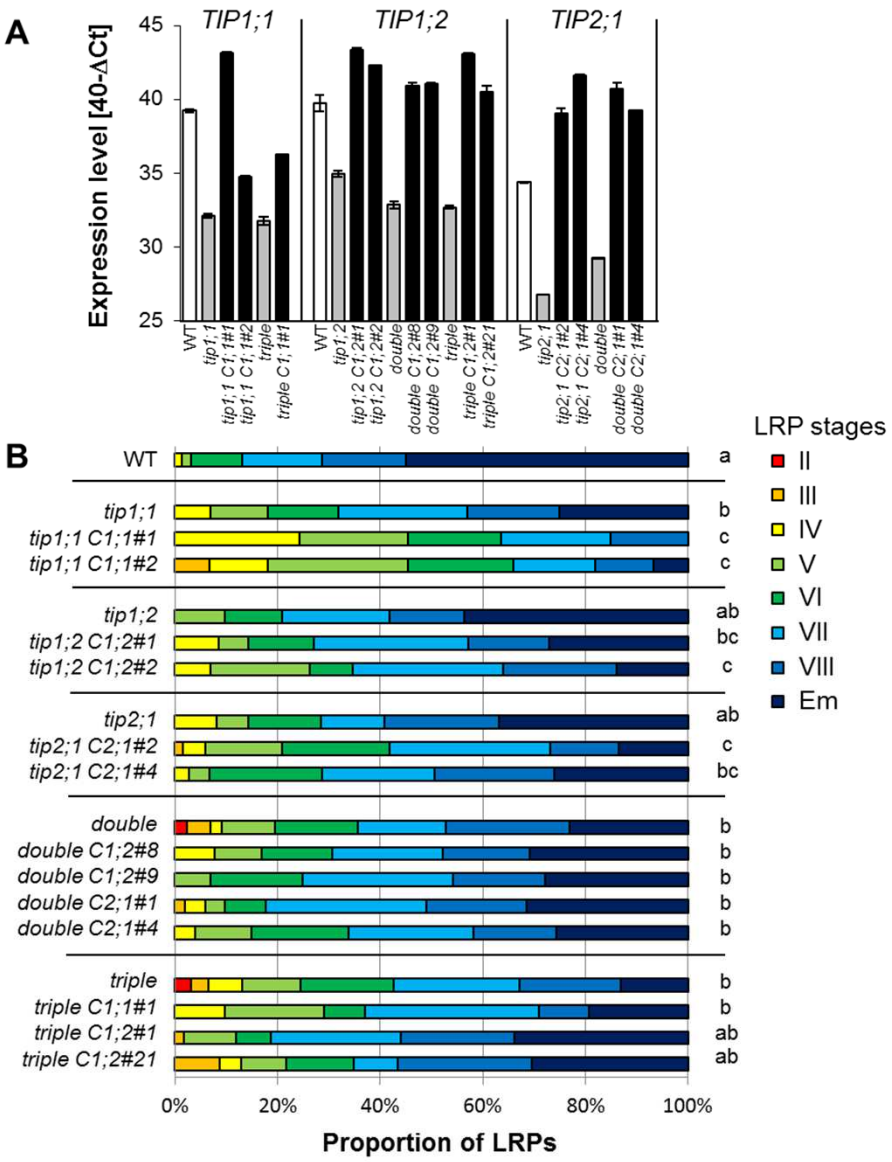

Figure 8. Constitutive expression of *AtTIP* genes in the *tip* mutant lines alters LRP development. A, Transgene *AtTIP* expression in the complemented *tip* mutant lines determined by RT-qPCR and compared to wild-type control. *Double*: *tip1;2* x *tip2;1*, *triple*: *tip1;1* x *tip1;2* x *tip2;1*. "*C*" indicates that the line is complemented, followed by the number of the *AtTIP* isoform and the number of the independently selected line. E.g. "*triple C1;2#21*" represents the *tip1;1* x *tip1;2* x *tip2;1* mutant complemented with *AtTIP1;2*, selected line no.21. B, Developmental stage distribution (from 2 to 8, Em: emerged; (Malamy and Benfey, 1987)) of LRP 42 h pgi in Arabidopsis *tip* mutant and the complemented lines. n = 23 - 102, pooled from two independent experiments. Statistical analysis was performed using standard contingency tables to sequentially compare relevant lines (see Materials and Methods). Only lines corresponding to one mutant line (grouped by horizontal lines in the chart) where compared with each other and the wild-type.

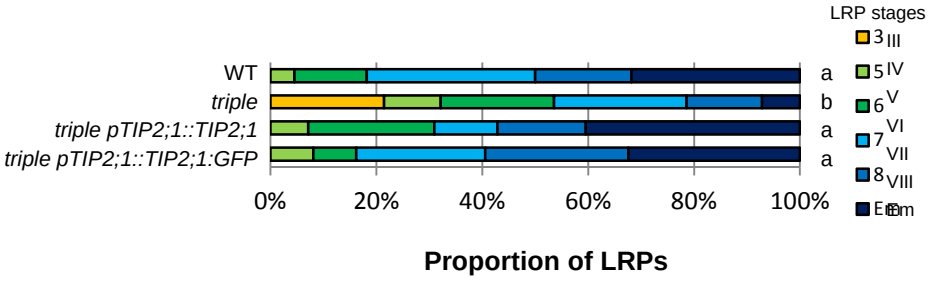

Figure 9. Expression of *AtTIP2;1* under the control of its own promoter rescues the LRE phenotype of the triple *tip* mutant. Developmental stage distribution (from III to VIII, Em: emerged; (Malamy and Benfey, 1997)) of LRP 42 h pgi from seedlings of wild type (WT), the *tip1;1 x tip1;2 x tip2;1* triple mutant (triple), transformed triple tip mutant with *p(promoter)TIP2;1::TIP2;1* or *pTIP2;1::TIP2;1:GFP* fusions lines. n = 22 – 38. Statistical analysis was performed using standard contingency tables to sequentially compare relevant lines (see Materials and Methods).

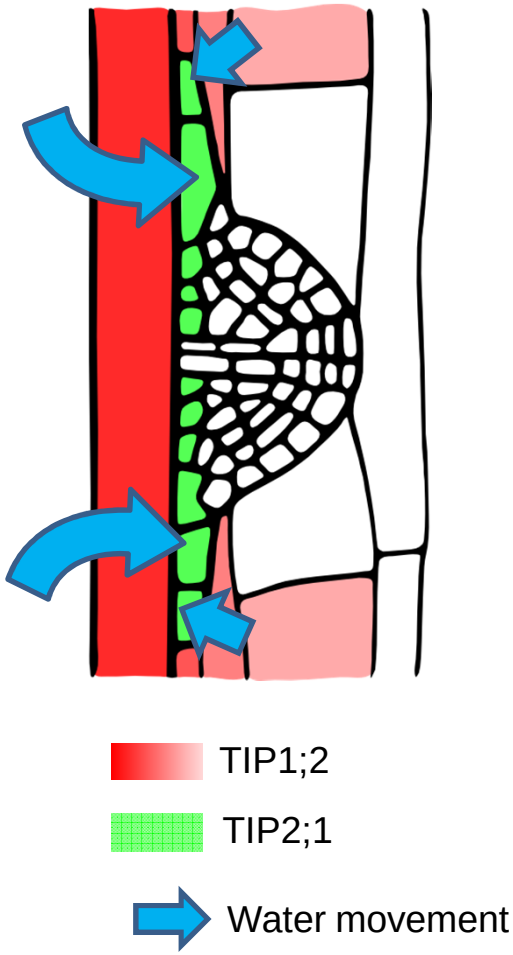

Figure 10. A tightly regulated TIP expression pattern is required for fast LRP development. After the LRP development is initialized, a gradient of TIP1;2 expression (red; dark: high expression, light: low expression) is observed from inner to outer root tissues and down-regulated in cortex cells facing the initialized LRP. At the same time, TIP2;1 expression (green) is up-regulated in cells located at the base of the LRP. This could result in a gradient in vacuolar water permeability between the base of the LRP on one side the LRP surrounding tissues on the other side. The cells at the base of the LRP therefore could expand rapidly and allow the fast growth and emergence of the LRP throughout the overlaying tissues.

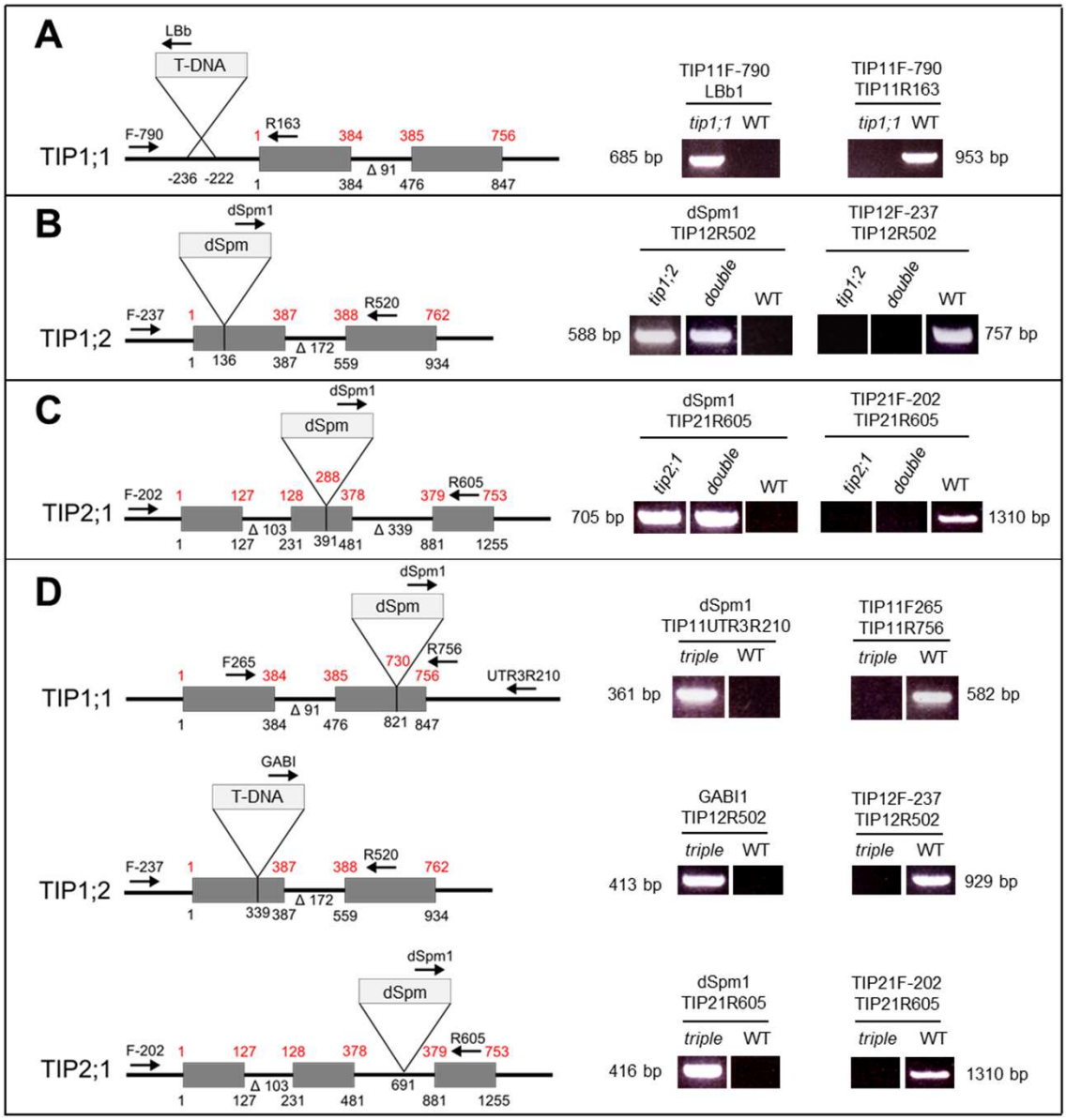

Supplemental Figure 1. Verification of the homozygosity of the insertion in the different *tip* mutant lines. Numbers in red and black indicate the position on the cDNA and the genomic DNA, respectively (position 1 starting at the start codon). Numbers on the primers refer to the cDNA positions. A, Insertion in the *tip1;1* single mutant. The T-DNA insertion induced the loss of 13 bp within the 5' non-coding region. B, Insertion in the *AtTIP1;2* gene of *tip1;2* single and *tip1;2 x tip2;1* double mutant. C, Insertion in the AtTIP2;1 gene of *tip2;*1 single and *tip1;2 x tip2;1* double mutant. D, Insertions in the *tip1;1 x tip1;2 x tip2;1* triple mutant. The left panels show the PCR analyses performed from the genomic DNA of the different wild-type and mutant lines using the indicated primers.

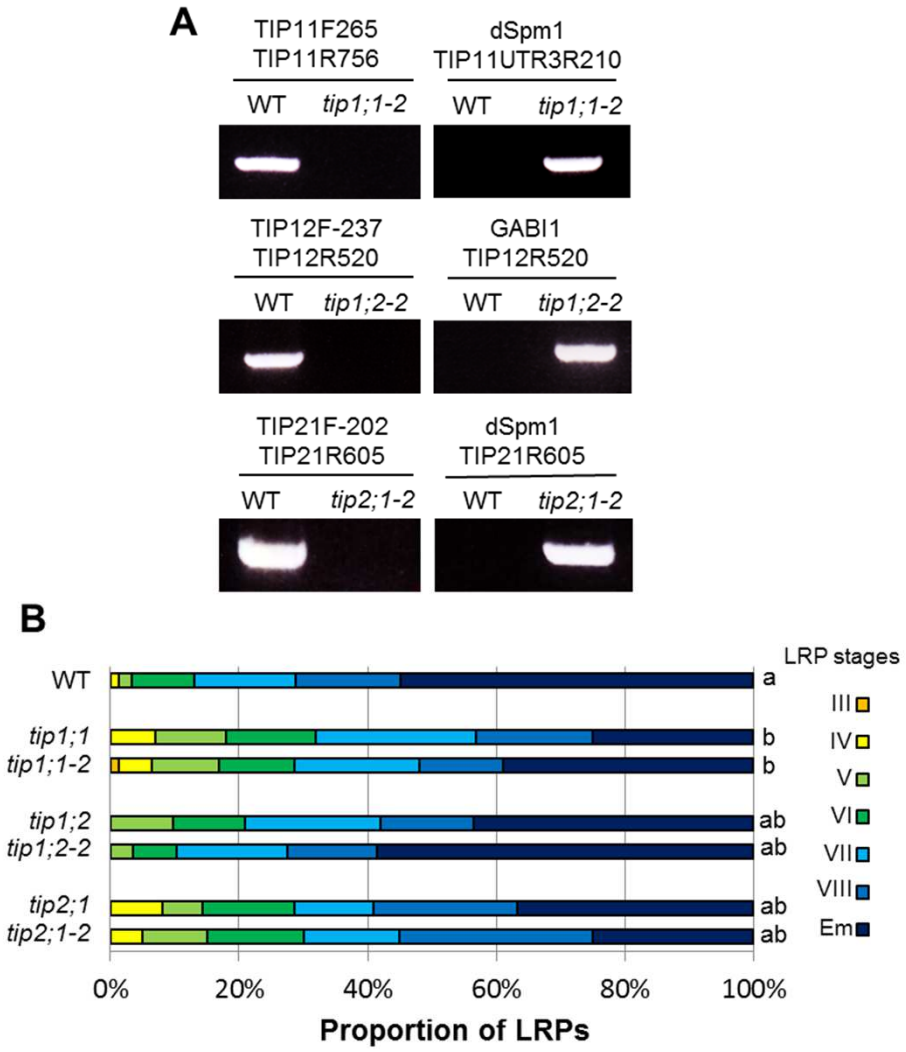

Supplemental Figure 2. Independent *tip* mutants exhibit delay in LRP development. A, Verification of the dSpm or T-DNA insertions in the second, independent batch of *tip* mutants: *tip1;1-2*, *tip1;2-2* (Schussler et al., 2008) and *tip2;1-2* (Schüssler and Schjoerring, unpublished data) by PCR using the primers given in Table1, according to the scheme shown in Figure 1. B, Developmental stage distribution (Developmental stage distribution (from III to VIII, Em: emerged; (Malamy and Benfey, 1997)) of LRP 42 h pgi. n = 20 – 77.Statistical analysis was performed using standard contingency tables to sequentially compare relevant lines (see Materials and Methods).

Parsed Citations

Agre P, Preston GM, Smith BL, Jung JS, Raina S, Moon C, Guggino WB, Nielsen S (1993) Aquaporin CHIP: the archetypal molecular water channel. Am J Physiol 265: F463-476

Pubmed: Author and Title
CrossRef: Author and Title
Google Scholar: Author Only Title Only Author and Title

Alexandersson E, Fraysse L, Sjovall-Larsen S, Gustavsson S, Fellert M, Karlsson M, Johanson U, Kjellbom P (2005) Whole gene family expression and drought stress regulation of aquaporins. Plant Molecular Biology 59: 469-484

Pubmed: Author and Title
CrossRef: Author and Title
Google Scholar: Author Only Title Only Author and Title

Alonso JM, Stepanova AN, Leisse TJ, Kim CJ, Chen H, Shinn P, Stevenson DK, Zimmerman J, Barajas P, Cheuk R, Gadrinab C, Heller C, Jeske A, Koesema E, Meyers CC, Parker H, Prednis L, Ansari Y, Choy N, Deen H, Geralt M, Hazari N, Hom E, Karnes M, Mulholland C, Ndubaku R, Schmidt I, Guzman P, Aguilar-Henonin L, Schmid M, Weigel D, Carter DE, Marchand T, Risseeuw E, Brogden D, Zeko A, Crosby WL, Berry CC, Ecker JR (2003) Genome-wide insertional mutagenesis of Arabidopsis thaliana. Science 301: 653-657

Pubmed: Author and Title
CrossRef: Author and Title
Google Scholar: Author Only Title Only Author and Title

Arvidsson S, Kwasniewski M, Riano-Pachon DM, Mueller-Roeber B (2008) QuantPrime--a flexible tool for reliable high-throughput primer design for quantitative PCR. BMC Bioinformatics 9: 465

Pubmed: Author and Title
CrossRef: Author and Title
Google Scholar: Author Only Title Only Author and Title

Barrieu F, Chaumont F, Chrispeels MJ (1998) High expression of the tonoplast aquaporin ZmTIP1 in epidermal and conducting tissues of maize. Plant Physiology 117: 1153-1163

Pubmed: Author and Title
CrossRef: Author and Title
Google Scholar: Author Only Title Only Author and Title

Beebo A, Thomas D, Der C, Sanchez L, Leborgne-Castel N, Marty F, Schoefs B, Bouhidel K (2009) Life with and without AtTIP1;1, an Arabidopsis aquaporin preferentially localized in the apposing tonoplasts of adjacent vacuoles. Plant Mol Biol 70: 193-209

Pubmed: Author and Title
CrossRef: Author and Title
Google Scholar: Author Only Title Only Author and Title

Bienert GP, Bienert MD, Jahn TP, Boutry M, Chaumont F (2011) Solanaceae XIPs are plasma membrane aquaporins that facilitate the transport of many uncharged substrates. Plant J 66: 306-317

Pubmed: Author and Title
CrossRef: Author and Title
Google Scholar: Author Only Title Only Author and Title

Bienert GP, Heinen RB, Berny MC, Chaumont F (2014) Maize plasma membrane aquaporin ZmPIP2;5, but not ZmPIP1;2, facilitates transmembrane diffusion of hydrogen peroxide. Biochim Biophys Acta 1838: 216-222

Pubmed: Author and Title
CrossRef: Author and Title
Google Scholar: Author Only Title Only Author and Title

Bienert GP, Moller ALB, Kristiansen KA, Schulz A, Moller IM, Schjoerring JK, Jahn TP (2007) Specific aquaporins facilitate the diffusion of hydrogen peroxide across membranes. Journal of Biological Chemistry 282: 1183-1192

Pubmed: Author and Title
CrossRef: Author and Title
Google Scholar: Author Only Title Only Author and Title

Bienert GP, Thorsen M, Schussler MD, Nilsson HR, Wagner A, Tamas MJ, Jahn TP (2008) A subgroup of plant aquaporins facilitate the bi-directional diffusion of As(OH)3 and Sb(OH)3 across membranes. BMC Biol 6: 26

Pubmed: Author and Title
CrossRef: Author and Title
Google Scholar: Author Only Title Only Author and Title

Bustin SA, Benes V, Garson JA, Hellemans J, Huggett J, Kubista M, Mueller R, Nolan T, Pfaffl MW, Shipley GL, Vandesompele J, Wittwer CT (2009) The MIQE guidelines: minimum information for publication of quantitative real-time PCR experiments. Clin Chem 55: 611-622

Pubmed: Author and Title
CrossRef: Author and Title
Google Scholar: Author Only Title Only Author and Title

Casimiro I, Marchant A, Bhalerao RP, Beeckman T, Dhooge S, Swarup R, Graham N, Inze D, Sandberg G, Casero PJ, Bennett M (2001) Auxin transport promotes Arabidopsis lateral root initiation. Plant Cell 13: 843-852

Pubmed: Author and Title
CrossRef: Author and Title
Google Scholar: Author Only Title Only Author and Title

Chaumont F, Barrieu F, Herman EM, Chrispeels MJ (1998) Characterization of a maize tonoplast aquaporin expressed in zones of

cell division and elongation. Plant Physiology 117: 1143-1152
Pubmed: Author and Title
CrossRef: Author and Title
Google Scholar: Author Only Title Only Author and Title

Chaumont F, Tyerman SD (2014) Aquaporins: highly regulated channels controlling plant water relations. Plant Physiol 164: 1600-1618
Pubmed: Author and Title
CrossRef: Author and Title
Google Scholar: Author Only Title Only Author and Title

Clough SJ, Bent AF (1998) Floral dip: a simplified method for Agrobacterium-mediated transformation of Arabidopsis thaliana. Plant J 16: 735-743
Pubmed: Author and Title
CrossRef: Author and Title
Google Scholar: Author Only Title Only Author and Title

Curtis MD, Grossniklaus U (2003) A gateway cloning vector set for high-throughput functional analysis of genes in planta. Plant Physiol 133: 462-469
Pubmed: Author and Title
CrossRef: Author and Title
Google Scholar: Author Only Title Only Author and Title

Daniels MJ, Chaumont F, Mirkov TE, Chrispeels MJ (1996) Characterization of a new vacuolar membrane aquaporin sensitive to mercury at a unique site. Plant Cell 8: 587-599
Pubmed: Author and Title
CrossRef: Author and Title
Google Scholar: Author Only Title Only Author and Title

Daniels MJ, Mirkov TE, Chrispeels MJ (1994) The plasma membrane of Arabidopsis thaliana contains a mercury- insensitive aquaporin that is a homolog of the tonoplast water channel protein TIP. Plant Physiol 106: 1325-1333
Pubmed: Author and Title
CrossRef: Author and Title
Google Scholar: Author Only Title Only Author and Title

De Smet I, Tetsumura T, De Rybel B, Frey NF, Laplaze L, Casimiro I, Swarup R, Naudts M, Vanneste S, Audenaert D, Inze D, Bennett MJ, Beeckman T (2007) Auxin-dependent regulation of lateral root positioning in the basal meristem of Arabidopsis. Development 134: 681-690
Pubmed: Author and Title
CrossRef: Author and Title
Google Scholar: Author Only Title Only Author and Title

De Smet I, White PJ, Bengough AG, Dupuy L, Parizot B, Casimiro I, Heidstra R, Laskowski M, Lepetit M, Hochholdinger F, Draye X, Zhang H, Broadley MR, Peret B, Hammond JP, Fukaki H, Mooney S, Lynch JP, Nacry P, Schurr U, Laplaze L, Benfey P, Beeckman T, Bennett M (2012) Analyzing lateral root development: how to move forward. Plant Cell 24: 15-20
Pubmed: Author and Title
CrossRef: Author and Title
Google Scholar: Author Only Title Only Author and Title

Ditengou FA, Teale WD, Kochersperger P, Flittner KA, Kneuper I, van der Graaff E, Nziengui H, Pinosa F, Li X, Nitschke R, Laux T, Palme K (2008) Mechanical induction of lateral root initiation in Arabidopsis thaliana. Proc Natl Acad Sci U S A 105: 18818-18823
Pubmed: Author and Title
CrossRef: Author and Title
Google Scholar: Author Only Title Only Author and Title

Dolan L, Janmaat K, Willemsen V, Linstead P, Poethig S, Roberts K, Scheres B (1993) Cellular organisation of the Arabidopsis thaliana root. Development 119: 71-84
Pubmed: Author and Title
CrossRef: Author and Title
Google Scholar: Author Only Title Only Author and Title

Dubrovsky JG, Rost TL, Colon-Carmona A, Doerner P (2001) Early primordium morphogenesis during lateral root initiation in Arabidopsis thaliana. Planta 214: 30-36
Pubmed: Author and Title
CrossRef: Author and Title
Google Scholar: Author Only Title Only Author and Title

Dubrovsky JG, Sauer M, Napsucialy-Mendivil S, Ivanchenko MG, Friml J, Shishkova S, Celenza J, Benkova E (2008) Auxin acts as a local morphogenetic trigger to specify lateral root founder cells. Proc Natl Acad Sci U S A 105: 8790-8794
Pubmed: Author and Title
CrossRef: Author and Title
Google Scholar: Author Only Title Only Author and Title

Eisenbarth DA, Weig AR (2005) Dynamics of aquaporins and water relations during hypocotyl elongation in Ricinus communis L. seedlings. Journal of Experimental Botany 56: 1831-1842
Pubmed: Author and Title
CrossRef: Author and Title
Google Scholar: Author Only Title Only Author and Title

Fricke W, Chaumont F (2007) Solute and water relations of growing plant cells. In JP Verbelen, K Vissenberg, eds, The expanding

cell, Vol 5. Springer, Berlin Heidelberg, pp 7-31
Pubmed: Author and Title
CrossRef: Author and Title
Google Scholar: Author Only Title Only Author and Title

Fricke W, Peters WS (2002) The biophysics of leaf growth in salt-stressed barley. A study at the cell level. Plant Physiology 129: 374-388
Pubmed: Author and Title
CrossRef: Author and Title
Google Scholar: Author Only Title Only Author and Title

Frigerio L, Hinz G, Robinson DG (2008) Multiple vacuoles in plant cells: rule or exception? Traffic 9: 1564-1570
Pubmed: Author and Title
CrossRef: Author and Title
Google Scholar: Author Only Title Only Author and Title

Gao YP, Young L, Bonham-Smith P, Gusta LV (1999) Characterization and expression of plasma and tonoplast membrane aquaporins in primed seed of Brassica napus during germination under stress conditions. Plant Mol Biol 40: 635-644
Pubmed: Author and Title
CrossRef: Author and Title
Google Scholar: Author Only Title Only Author and Title

Gattolin S, Sorieul M, Hunter PR, Khonsari RH, Frigerio L (2009) In vivo imaging of the tonoplast intrinsic protein family in Arabidopsis roots. BMC Plant Biol 9: 133
Pubmed: Author and Title
CrossRef: Author and Title
Google Scholar: Author Only Title Only Author and Title

Gendreau E, Traas J, Desnos T, Grandjean O, Caboche M, Hofte H (1997) Cellular basis of hypocotyl growth in Arabidopsis thaliana. Plant Physiol 114: 295-305
Pubmed: Author and Title
CrossRef: Author and Title
Google Scholar: Author Only Title Only Author and Title

Gerbeau P, Guclu J, Ripoche P, Maurel C (1999) Aquaporin Nt-TIPa can account for the high permeability of tobacco cell vacuolar membrane to small neutral solutes. Plant J 18: 577-587
Pubmed: Author and Title
CrossRef: Author and Title
Google Scholar: Author Only Title Only Author and Title

Gomes D, Agasse A, Thiebaud P, Delrot S, Geros H, Chaumont F (2009) Aquaporins are multifunctional water and solute transporters highly divergent in living organisms. Biochim Biophys Acta 1788: 1213-1228
Pubmed: Author and Title
CrossRef: Author and Title
Google Scholar: Author Only Title Only Author and Title

Hachez C, Moshelion M, Zelazny E, Cavez D, Chaumont F (2006) Localization and quantification of plasma membrane aquaporin expression in maize primary root: a clue to understanding their role as cellular plumbers. Plant Mol Biol 62: 305-323
Pubmed: Author and Title
CrossRef: Author and Title
Google Scholar: Author Only Title Only Author and Title

Heinen RB, Ye Q, Chaumont F (2009) Role of aquaporins in leaf physiology. Journal of Experimental Botany 60: 2971-2985
Pubmed: Author and Title
CrossRef: Author and Title
Google Scholar: Author Only Title Only Author and Title

Higuchi T, Suga S, Tsuchiya T, Hisada H, Morishima S, Okada Y, Maeshima M (1998) Molecular cloning, water channel activity and tissue specific expression of two isoforms of radish vacuolar aquaporin. Plant And Cell Physiology 39: 905-913
Pubmed: Author and Title
CrossRef: Author and Title
Google Scholar: Author Only Title Only Author and Title

Hunter PR, Craddock CP, Di Benedetto S, Roberts LM, Frigerio L (2007) Fluorescent reporter proteins for the tonoplast and the vacuolar lumen identify a single vacuolar compartment in Arabidopsis cells. Plant Physiol 145: 1371-1382
Pubmed: Author and Title
CrossRef: Author and Title
Google Scholar: Author Only Title Only Author and Title

Jahn TP, Moller AL, Zeuthen T, Holm LM, Klaerke DA, Mohsin B, Kuhlbrandt W, Schjoerring JK (2004) Aquaporin homologues in plants and mammals transport ammonia. FEBS Lett 574: 31-36
Pubmed: Author and Title
CrossRef: Author and Title
Google Scholar: Author Only Title Only Author and Title

Jauh GY, Fischer AM, Grimes HD, Ryan CA, Rogers JC (1998) delta-Tonoplast intrinsic protein defines unique plant vacuole functions. Proceedings of the National Academy of Sciences of the United States of America 95: 12995-12999
Pubmed: Author and Title
CrossRef: Author and Title
Google Scholar: Author Only Title Only Author and Title

Johanson U, Karlsson M, Johansson I, Gustavsson S, Sjovall S, Fraysse L, Weig AR, Kjellbom P (2001) The complete set of genes encoding major intrinsic proteins in Arabidopsis provides a framework for a new nomenclature for major intrinsic proteins in plants. Plant Physiology 126: 1358-1369
Pubmed: Author and Title
CrossRef: Author and Title
Google Scholar: Author Only Title Only Author and Title

Kammerloher W, Fischer U, Piechottka GP, Schaffner AR (1994) Water channels in the plant plasma membrane cloned by immunoselection from a mammalian expression system. Plant J. 6: 187-199.
Pubmed: Author and Title
CrossRef: Author and Title
Google Scholar: Author Only Title Only Author and Title

Kumpf RP, Shi CL, Larrieu A, Sto IM, Butenko MA, Peret B, Riiser ES, Bennett MJ, Aalen RB (2013) Floral organ abscission peptide IDA and its HAE/HSL2 receptors control cell separation during lateral root emergence. Proc Natl Acad Sci U S A 110: 5235-5240
Pubmed: Author and Title
CrossRef: Author and Title
Google Scholar: Author Only Title Only Author and Title

Laskowski M, Biller S, Stanley K, Kajstura T, Prusty R (2006) Expression profiling of auxin-treated Arabidopsis roots: toward a molecular analysis of lateral root emergence. Plant Cell Physiol 47: 788-792
Pubmed: Author and Title
CrossRef: Author and Title
Google Scholar: Author Only Title Only Author and Title

Liu LH, Ludewig U, Gassert B, Frommer WB, von Wiren N (2003) Urea transport by nitrogen-regulated tonoplast intrinsic proteins in Arabidopsis. Plant Physiol 133: 1220-1228
Pubmed: Author and Title
CrossRef: Author and Title
Google Scholar: Author Only Title Only Author and Title

Lucas M, Godin C, Jay-Allemand C, Laplaze L (2008) Auxin fluxes in the root apex co-regulate gravitropism and lateral root initiation. J Exp Bot 59: 55-66
Pubmed: Author and Title
CrossRef: Author and Title
Google Scholar: Author Only Title Only Author and Title

Lucas M, Kenobi K, von Wangenheim D, Vobeta U, Swarup K, De Smet I, Van Damme D, Lawrence T, Peret B, Moscardi E, Barbeau D, Godin C, Salt D, Guyomarc'h S, Stelzer EH, Maizel A, Laplaze L, Bennett MJ (2013) Lateral root morphogenesis is dependent on the mechanical properties of the overlaying tissues. Proc Natl Acad Sci U S A 110: 5229-5234
Pubmed: Author and Title
CrossRef: Author and Title
Google Scholar: Author Only Title Only Author and Title

Ludevid D, Hofte H, Himelblau E, Chrispeels MJ (1992) The expression pattern of the tonoplast intrinsic protein gamma-TIP in Arabidopsis thaliana is correlated with cell enlargement. Plant Physiology 100: 1633-1639
Pubmed: Author and Title
CrossRef: Author and Title
Google Scholar: Author Only Title Only Author and Title

Macgregor DR, Deak KI, Ingram PA, Malamy JE (2008) Root system architecture in Arabidopsis grown in culture is regulated by sucrose uptake in the aerial tissues. Plant Cell 20: 2643-2660
Pubmed: Author and Title
CrossRef: Author and Title
Google Scholar: Author Only Title Only Author and Title

Malamy JE, Benfey PN (1997) Organization and cell differentiation in lateral roots of Arabidopsis thaliana. Development 124: 33-44
Pubmed: Author and Title
CrossRef: Author and Title
Google Scholar: Author Only Title Only Author and Title

Maurel C (1997) Aquaporins and water permeability of plant membranes. Annual Review of Plant Physiology and Plant Molecular Biology 48: 399-429
Pubmed: Author and Title
CrossRef: Author and Title
Google Scholar: Author Only Title Only Author and Title

Maurel C, Kado RT, Guern J, Chrispeels MJ (1995) Phosphorylation regulates the water channel activity of the seed- specific aquaporin alpha-TIP. Embo J. 14: 3028-3035
Pubmed: Author and Title
CrossRef: Author and Title
Google Scholar: Author Only Title Only Author and Title

Maurel C, Reizer J, Schroeder JI, Chrispeels MJ (1993) The vacuolar membrane protein gamma-TIP creates water specific channels in Xenopus oocytes. Embo Journal 12: 2241-2247
Pubmed: Author and Title
CrossRef: Author and Title
Google Scholar: Author Only Title Only Author and Title

Maurel C, Tacnet F, Guclu J, Guern J, Ripoche P (1997) Purified vesicles of tobacco cell vacuolar and plasma membranes exhibit

dramatically different water permeability and water channel activity. Proc Natl Acad Sci U S A 94: 7103-7108
Pubmed: Author and Title
CrossRef: Author and Title
Google Scholar: Author Only Title Only Author and Title

Maurel C, Verdoucq L, Luu DT, Santoni V (2008) Plant aquaporins: membrane channels with multiple integrated functions. Annual Review of Plant Biology 59: 595-624
Pubmed: Author and Title
CrossRef: Author and Title
Google Scholar: Author Only Title Only Author and Title

Morillon R, Lassalles JP (1999) Osmotic water permeability of isolated vacuoles. Planta 210: 80-84
Pubmed: Author and Title
CrossRef: Author and Title
Google Scholar: Author Only Title Only Author and Title

Nakagawa T, Kurose T, Hino T, Tanaka K, Kawamukai M, Niwa Y, Toyooka K, Matsuoka K, Jinbo T, Kimura T (2007) Development of series of gateway binary vectors, pGWBs, for realizing efficient construction of fusion genes for plant transformation. J Biosci Bioeng 104: 34-41
Pubmed: Author and Title
CrossRef: Author and Title
Google Scholar: Author Only Title Only Author and Title

Niemietz CM, Tyerman SD (1997) Characterization of Water Channels in Wheat Root Membrane Vesicles. Plant Physiol 115: 561-567
Pubmed: Author and Title
CrossRef: Author and Title
Google Scholar: Author Only Title Only Author and Title

Nour-Eldin HH, Hansen BG, Norholm MH, Jensen JK, Halkier BA (2006) Advancing uracil-excision based cloning towards an ideal technique for cloning PCR fragments. Nucleic Acids Res 34: e122
Pubmed: Author and Title
CrossRef: Author and Title
Google Scholar: Author Only Title Only Author and Title

Okubo-Kurihara E, Sano T, Higaki T, Kutsuna N, Hasezawa S (2009) Acceleration of vacuolar regeneration and cell growth by overexpression of an aquaporin NtTIP1;1 in tobacco BY-2 cells. Plant Cell Physiol 50: 151-160
Pubmed: Author and Title
CrossRef: Author and Title
Google Scholar: Author Only Title Only Author and Title

Peret B, De Rybel B, Casimiro I, Benkova E, Swarup R, Laplaze L, Beeckman T, Bennett MJ (2009) Arabidopsis lateral root development: an emerging story. Trends Plant Sci 14: 399-408
Pubmed: Author and Title
CrossRef: Author and Title
Google Scholar: Author Only Title Only Author and Title

Peret B, Li G, Zhao J, Band LR, Voss U, Postaire O, Luu DT, Da Ines O, Casimiro I, Lucas M, Wells DM, Lazzerini L, Nacry P, King JR, Jensen OE, Schaffner AR, Maurel C, Bennett MJ (2012) Auxin regulates aquaporin function to facilitate lateral root emergence. Nat Cell Biol 14: 991-998
Pubmed: Author and Title
CrossRef: Author and Title
Google Scholar: Author Only Title Only Author and Title

Petricka JJ, Winter CM, Benfey PN (2012) Control of Arabidopsis root development. Annu Rev Plant Biol 63: 563-590
Pubmed: Author and Title
CrossRef: Author and Title
Google Scholar: Author Only Title Only Author and Title

Raz V, Koornneef M (2001) Cell division activity during apical hook development. Plant Physiol 125: 219-226
Pubmed: Author and Title
CrossRef: Author and Title
Google Scholar: Author Only Title Only Author and Title

Reisen D, Leborgne-Castel N, Ozalp C, Chaumont F, Marty F (2003) Expression of a cauliflower tonoplast aquaporin tagged with GFP in tobacco suspension cells correlates with an increase in cell size. Plant Mol Biol 52: 387-400
Pubmed: Author and Title
CrossRef: Author and Title
Google Scholar: Author Only Title Only Author and Title

Richter GL, Monshausen GB, Krol A, Gilroy S (2009) Mechanical stimuli modulate lateral root organogenesis. Plant Physiol 151: 1855-1866
Pubmed: Author and Title
CrossRef: Author and Title
Google Scholar: Author Only Title Only Author and Title

Schunmann PHD, Ougham HJ (1996) Identification of three cDNA clones expressed in the leaf extension zone and with altered patterns of expression in the slender mutant of barley: A tonoplast intrinsic protein, a putative structural protein and protochlorophyllide oxidoreductase. Plant Molecular Biology 31: 529-537
Pubmed: Author and Title
CrossRef: Author and Title
Google Scholar: Author Only Title Only Author and Title

Schussler MD, Alexandersson E, Bienert GP, Kichey T, Laursen KH, Johanson U, Kjellbom P, Schjoerring JK, Jahn TP (2008) The effects of the loss of TIP1;1 and TIP1;2 aquaporins in Arabidopsis thaliana. Plant J 56: 756-767
Pubmed: Author and Title
CrossRef: Author and Title
Google Scholar: Author Only Title Only Author and Title

Soto G, Alleva K, Mazzella MA, Amodeo G, Muschietti JP (2008) AtTIP1;3 and AtTIP5;1, the only highly expressed Arabidopsis pollen-specific aquaporins, transport water and urea. FEBS Lett 582: 4077-4082
Pubmed: Author and Title
CrossRef: Author and Title
Google Scholar: Author Only Title Only Author and Title

Suga S, Imagawa S, Maeshima M (2001) Specificity of the accumulation of mRNAs and proteins of the plasma membrane and tonoplast aquaporins in radish organs. Planta 212: 294-304.
Pubmed: Author and Title
CrossRef: Author and Title
Google Scholar: Author Only Title Only Author and Title

Swarup K, Benkova E, Swarup R, Casimiro I, Peret B, Yang Y, Parry G, Nielsen E, De Smet I, Vanneste S, Levesque MP, Carrier D, James N, Calvo V, Ljung K, Kramer E, Roberts R, Graham N, Marillonnet S, Patel K, Jones JD, Taylor CG, Schachtman DP, May S, Sandberg G, Benfey P, Friml J, Kerr I, Beeckman T, Laplaze L, Bennett MJ (2008) The auxin influx carrier LAX3 promotes lateral root emergence. Nat Cell Biol 10: 946-954
Pubmed: Author and Title
CrossRef: Author and Title
Google Scholar: Author Only Title Only Author and Title

Tissier AF, Marillonnet S, Klimyuk V, Patel K, Torres MA, Murphy G, Jones JD (1999) Multiple independent defective suppressor-mutator transposon insertions in Arabidopsis: a tool for functional genomics. Plant Cell 11: 1841-1852
Pubmed: Author and Title
CrossRef: Author and Title
Google Scholar: Author Only Title Only Author and Title

Uehlein N, Lovisolo C, Siefritz F, Kaldenhoff R (2003) The tobacco aquaporin NtAQP1 is a membrane CO2 pore with physiological functions. Nature 425: 734-737
Pubmed: Author and Title
CrossRef: Author and Title
Google Scholar: Author Only Title Only Author and Title

Vander Willigen C, Postaire O, Tournaire-Roux C, Boursiac Y, Maurel C (2006) Expression and inhibition of aquaporins in germinating Arabidopsis seeds. Plant Cell Physiol 47: 1241-1250
Pubmed: Author and Title
CrossRef: Author and Title
Google Scholar: Author Only Title Only Author and Title

Weig A, Deswarte C, Chrispeels MJ (1997) The major intrinsic protein family of Arabidopsis has 23 members that form three distinct groups with functional aquaporins in each group. Plant Physiol 114: 1347-1357
Pubmed: Author and Title
CrossRef: Author and Title
Google Scholar: Author Only Title Only Author and Title

Wudick MM, Luu DT, Tournaire-Roux C, Sakamoto W, Maurel C (2014) Vegetative and sperm cell-specific aquaporins of Arabidopsis highlight the vacuolar equipment of pollen and contribute to plant reproduction. Plant Physiol 164: 1697-1706
Pubmed: Author and Title
CrossRef: Author and Title
Google Scholar: Author Only Title Only Author and Title

Zar JH (2010) Biostatistical Analysis, Ed 5th Edition. Pearson Prentice-Hall, Upper Saddle River, NJ.
Pubmed: Author and Title
CrossRef: Author and Title
Google Scholar: Author Only Title Only Author and Title